HOLOGRAPHIC DIELECTRIC GRATINGS: THEORY AND PRACTICE

Thesis by

Milton M. T. Chang

In Partial Fulfillment of the Requirements

For the Degree of

Doctor of Philosophy

California Institute of Technology

Pasadena, California

1969

(Submitted May 23, 1969)

ACKNOWLEDGEMENTS

After spending some 85% of my life in school, there are many teachers and colleagues whose influence I would like to acknowledge.

First, I would like to thank my adviser, Professor Nicholas George, for his advice and encouragement during my studies at Caltech. His understanding and personal attention to each student were found to be most valuable, especially at moments of frustration. His emphasis on attacking a problem from a fundamental point of view, such as " Let us see how each grain scatters", has inspired the work described in the pages that follow.

I would like to thank my colleague and friend, John T. McCrickerd, for the stimulating discussions on various subjects related to holography, and for setting an example in doing things precisely and patiently. Thanks are also due to a student in holography of an earlier generation, Dr. John W. Matthews.

My gratitude extends to my high school teachers, the Marist Brothers, who have devoted themselves to education. In particular, it was Brother Kenny and Brother Bosco who first aroused my interest in science.

I am grateful to Mrs. Ruth Stratton for typing my thesis and so expertly putting it in the correct form, Miss Kikuko Matsumoto and Mrs. Edith Huang for their valuable assistance with the computer programming, and Paula Samazan for her eagerness to help in obtaining references.

I am thankful for the financial assistance of the Air Force Office of Scientific Research in their partial support of this work.

HOLOGRAPHIC DIELECTRIC GRATING: THEORY AND PRACTICE

Milton M. T. Chang

ABSTRACT

A holographic dielectric grating is a diffraction grating comprised of a periodic variation of the refractive index of a medium, and is produced by the interference pattern of two monochromatic waves. Emphasis is placed upon photographic emulsion as the medium for recording the pattern, but the treatment is general and includes any material that can have an internal modulation of the refractive index. Three topics are treated: the effective dielectric constant of the emulsion, the diffraction of light by dielectric gratings, and the techniques for producing gratings with high efficiency and good resolution.

The photographic emulsion is treated as an artificially loaded material, i.e. as a suspension of grains in a gelatin base. A Mie scattering theory analysis is used and the effect of adjacent scatterers on the local field is accounted for by the Lorentz-Lorenz relation. The optical density of the emulsion is shown to be proportional to the number of grains present. The effective index variation after bleaching is proportional to the pre-bleached optical density, which implies that the emulsion should have a linear density vs. exposure curve to effect a sinusoidally modulated index of refraction. A relation between the modulation transfer function (MTF) of bleached and unbleached emulsion is derived. Means for improvement of the MTF is also obtained analytically.

The diffraction of light by a dielectric grating is analyzed using the Raman-Nath formalism which is generalized to include loss. Graphs are presented showing the diffraction efficiency versus the index modulation for a wide range of thicknesses and loss. The peak efficiency for arbitrary emulsion thickness can be obtained from measurements at a specific thickness. The conclusion is reached that presently available emulsion should be made thicker, preferably in the 20-30 micron range.

The basic physical processes of various holographic materials are described. The processing techniques of photographic emulsion are emphasized and the merits of various bleaches are evaluated. It is found that resolution can be increased by using a reversal process. The dielectric grains in an emulsion processed this way are round in shape. A desensitizing dye can be used to stabilize the grains. A method of extending the dynamic range of the photographic emulsion using a pre-flashing exposure technique is also described.

Several experiments are proposed, and recommendations are made which may serve as guide-lines for the development of more suitable materials for holographic recording.

TABLE OF CONTENTS

INTRODUCTION

The term dielectric grating has been widely applied to gratings which are produced holographically, i.e., the interference pattern of two monochromatic plane waves are recorded in a medium, so that a periodic variation of the amplitude transmittance or index of refraction results. Better holographic materials and more powerful lasers are now available, so that large gratings of excellent quality can be produced commercially and the more general forms of gratings, such as Fresnel zone plates, can be used to replace conventional optical elements.

Our main interest is to gain some insight into the diffraction process of holographically produced gratings. To do so, three separate topics must be studied. These are the diffraction problem for a dielectric grating with a sinusoidally modulated index of refraction, an appropriate formulation of the effective index of refraction, and the techniques for producing such gratings with the specifications obtained from the first two topics. In this study, we placed our emphasis on photographic emulsion which is the most commonly used material, but with slight modification the problems treated here are applicable to any materials that have an internal index modulation.

We start by giving a survey of the materials that are now available and the basic processes of image formation and chemical treatments of photographic emulsions. Specific recommendations are made to improve the linearity and decrease the scattering noise of the commercially available emulsions. A formulation of the index of refraction of bleached emulsion is derived, and the result is correlated to the pre-bleaching density. This is necessary because it is difficult

to measure the small index change. We have also included in this formulation the modulation of the index of refraction for each spatial frequency, and related that to the pre-bleaching modulation transfer function. From this method of presenting the index of refraction, we can immediately see that it is possible to improve the modulation at a particular spatial frequency to unity. This opens the possibility of producing gratings with extremely small line spacing which could not otherwise be produced even at great expense. In relating the index change to its pre-bleaching density, we are able to specify the required characteristic curve for an emulsion that will enable one to produce a truly sinusoidally modulated index of refraction. In Chapter 3, the diffraction of light by a dielectric grating is analyzed using the Raman-Nath formalism which is generalized to include loss. With specific parameters encountered in holographic materials, the coupled wave equations are solved using a digital computer. A significant result obtained is the determination of the maximum diffraction efficiency obtainable for a lossy grating with a fixed thickness. In Chapter 4, the results obtained are correlated and the specific recommendations made can serve as a guide-line for photographic chemists to develop the most desirable emulsions.

CHAPTER ONE

HOLOGRAPHIC MATERIAL

1.1 Introduction

Material that can be used for holographic recording must satisfy two basic needs. It must at least be able to resolve fringes of a few wavelengths' separation and it must be able to retain the information recorded while interrogation takes place. Ideally though, the requirements are: (1) Infinite resolution for high density information storage without grain noise, (2) Dimensional stability so that a faithful reproduction of the original wave-front results, (3) Real time recording without processing, which can be erased for future use, (4) Losslessness so that highly efficient reconstruction can result, (5) No thickness limitation so that storage capacity can be increased. These are just a few requirements that present day applications of holography call for. As new applications for holography are discovered other requirements may become more apparent.

At present, many holographic materials are available, but none satisfies all of the above requirements. The most commonly used is the photographic emulsion. Other materials are photochromic materials, photosensitive plastics, ferroelectric crystals, photoresists, thermal plastics, dichromated gelatin and photopolymer systems. In this chapter, the characteristics of each material in relation to holographic applications will be described briefly, and the description of photographic film will be given in more detail. The significant contribution described in this chapter is that we have found,by pre-flashing the film plates with a short burst of light, we are able to increase

both the linearity and the dynamic range of the film. Another significant result is the use of reversal process to increase the quality of the gratings produced and one such process is described here. This reversal process differs in principle from the normal process, which involves either bleaching or tanning (1.1). Stabilization of the final grating using desensitizing dye is described here for the first time. A numerical method of fitting the H-D curve is also given in this chapter.

1.2 Photographic Emulsions

Photographic emulsion is most commonly used for holographic recording because it can be used over a wide spectral range with relatively high sensitivity. It can resolve approximately 3000 lines/mm and,when processed properly, it has very low loss so that high diffraction efficiency is made possible. The disadvantages of using photographic emulsion are that it requires processing, is not reusable, lacks dimensional stability, has grain noise, and is limited to thicknesses of less than 50 microns for uniform processing. The resolution and thickness of a few commercially available films used for holography are listed in Table 1.1. A good reference book for various aspects of photographic emulsion is a text by Mees and James (1.2). The two volumes on photographic chemistry by Glafkides are found to be

---

1.1 "Methods of producing phase holograms with conventional photographic materials", Prepared by Special Applications, Eastman Kodak Company, Rochester, N.Y. 1968.

1.2 C. E. Mees, T. H. James, The Theory of Photographic Process, Mac Millan Company, 3rd Edition 1966.

TABLE 1.1

FILM TYPE	RESOLUTION	EMULSION THICKNESS
Kodak 649-F	> 3000 lines/mm	17μ 6μ film
Kodak High Resolution Plates	> 3000 lines/mm	9μ 6μ film
Kodak SO-243	500 lines/mm	4μ
Kodak High Contrast Copy	250 lines/mm	6-8μ
Agfa (1.4) 14C70, 14C75	1500 lines/mm	4μ
Agfa 14E56, 14E70, 14E75	2800 lines/mm	6μ
Agfa, 8E56, 8E70, 8E75	3000 lines/mm	6μ

(1.4) D. Schultze, Laser Focus 4, 23 (1968)

most valuable (1.3).

Photographic emulsion is a colloidal suspension of small silver halide crystals in gelatin. A typical emulsion contains 20 - 40% by weight, 5 - 10% by volume, of silver halide crystals, although the specific amount for each emulsion is not generally known. After being exposed to light, it has to be processed before it can be displayed. Processing involves a combination of development, stop, fix, wash, bleach, wash and rinse. Each of these steps will be described below.

1.2.1 Exposure

When photographic film is used for picture taking, the speed of the film is rated by its ASA number, from which one can compute the relative exposure requirement of two different films. In most cases, holographic recording is done with a single spectral line from a laser, thus the ASA number becomes meaningless, because it is standardized with daylight exposure. In addition, the neutral density of the processed holographic film is so high compared to that of ordinary films that the ASA number, a guide number determined for density between 0.1 to 0.8 above fog, is not very reliable. In short, the relative speed of different films must be determined experimentally and specifically for each wavelength.

During exposure, a latent image is formed in the silver halide crystals. The theory of latent image formation is a controversial one

---

1.3 P. Glafkides, Photographic Chemistry, Vol. 1,2, Fountain Press, London, 1960.

and the commonly accepted theory has been put forth by Mott and Gurney (1.5). They assumed that sensitive specks are present on the surface of the crystal; they can be either metallic silver or silver sulfide. When a photon is absorbed by the silver halide crystal, a halide ion becomes a free electron and a halide atom. The electron is free to move about inside the crystal and will eventually hit the sensitive speck and get trapped. Trapping is possible because the conduction band of the crystal is at a higher level than that of the metallic silver. After collecting an electron, the silver speck becomes negatively charged and sets up an electric field. Since the positive ion is free to move about in a silver halide crystal which is an ionic crystal, it is attracted by the field and moves toward the negatively charged speck. As more photons are absorbed, more silver atoms will aggregate at the surface of the crystal. There is a balance of neutral halide atoms. They are not very mobile, but are able to exchange electrons with neighboring halide ions and move effectively to the surface of the crystal to be absorbed by the constituents in the gelatin.

It has been determined experimentally that a grain can be developed only after any speck has collected four or more silver atoms, and in most cases, the whole grain is developed. The quantum yield (number of silver atoms obtained per absorbed photon) is approximately 10^8, since each grain contains about 10^9 silver atoms. If we assume

---

1.5 N. F. Mott and R. W. Gurney, Electronic Processes in Ionic Crystals, Oxford Press, London 1957.

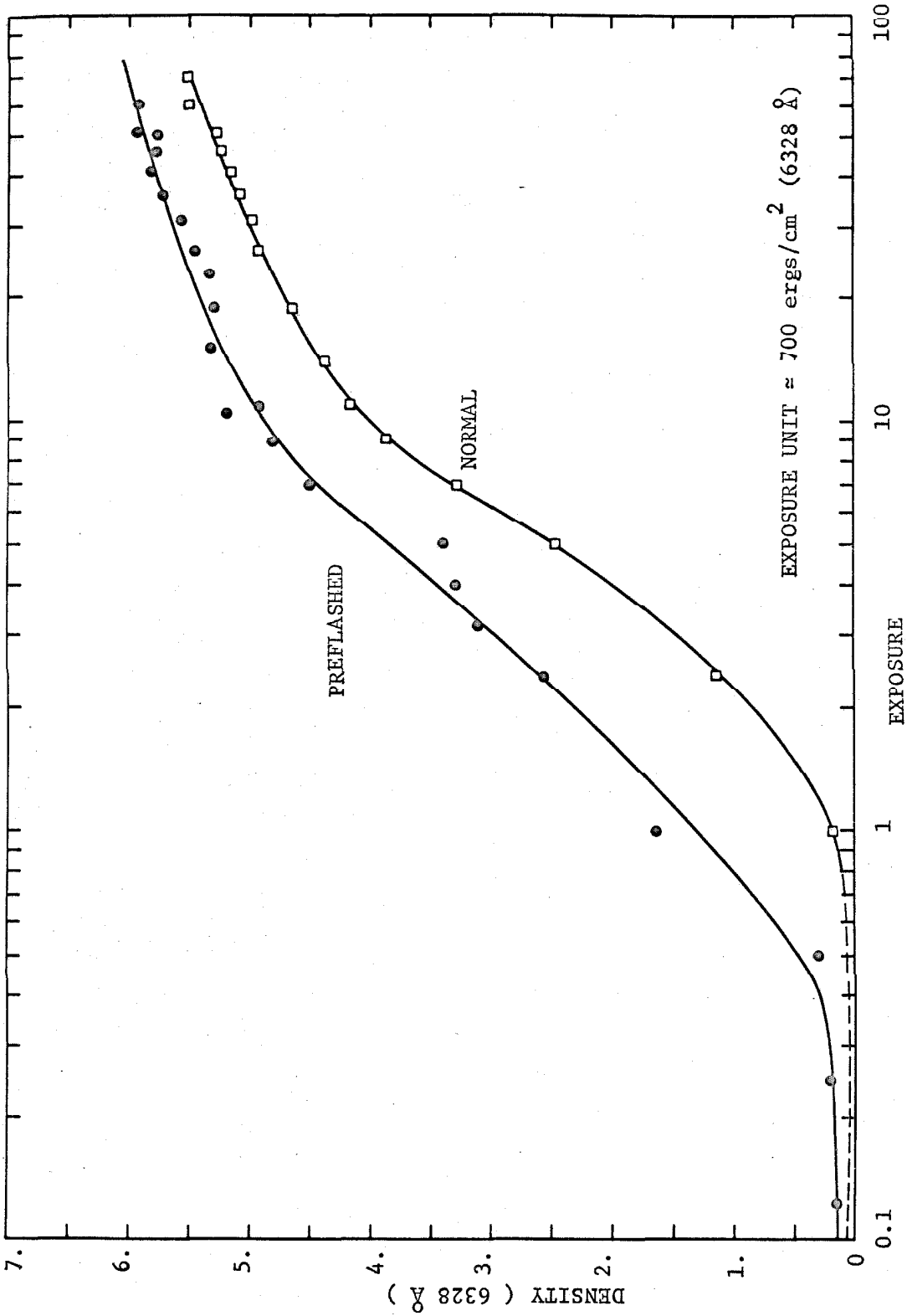

FIGURE 1.1 H-D CURVES OF NORMAL AND PREFLASHED 649F PLATES

that 1% of the incident photon is absorbed, then the overall quantum yield is between 10^5 and 10^6.

The characteristic of a given emulsion is often described by the Herter-Dreffield curve (H-D curve); that is, the density of the emulsion is plotted against the logarithm of the exposure. It is found by Wyant (1.6) that by pre-flashing the plates, one is able to increase the slope of the H-D curve at the lower portion of the H-D curve. This method, and baking of the plates, have long been used by astronomers as standard practices to compensate for the reciprocity failure. A comprehensive discussion is given by Miller (1.7).

We have pre-flashed the 649-F plates with an electronic flash to a neutral density of 0.15 before exposure. Plots of the H-D curves for the flashed and unflashed plates are shown in Figure 1.1. We see that there is a slight decrease in the gamma for the pre-flashed plates. A more important difference is that the pre-flashed plate has a larger region of constant slope, which means that it has a wider dynamic range. We also see that it can reach a higher ultimate density.

These observations can be explained simply in the following manner. As we have mentioned before, a grain could be developed only if a speck has more than 3 or 4 silver atoms. By flashing the plates, we distribute one or two silver atoms in most of the grains, therefore they can be developed after absorbing fewer additional photons. It has

---

1.6 J. C. Wyant and M. P. Givens, J. Opt. Soc. Am. 58, 357 (1968).

1.7 W. C. Miller, Publications of the Astronomical Soc. of the Pacific 76, 328 (1964).

been shown by Frieser (1.8), using statistical methods, that the H-D curve shifts in the manner shown in Figure 1.1 when less photons are needed to initiate development.

The difference in the ultimate density is due to the fact that only a limited number of grains will be developed during the short development time. Certain small grains that would not normally be developed during this period for the unflashed plates are now developed. This causes the ultimate density to increase. This fact may also be part of the reason the H-D curve has a smaller gamma. It has been shown by Frieser that an emulsion with grains of more uniform size has a higher gamma.

We note that the points did not fit the curves very well. This is attributed to the mechanical shutter used to expose the plates, which is not a very accurate and reliable timing device.

Figure 1.2 is another H-D curve for 649-F film, which has been developed in a special spray developer. The solid curve is obtained by a device designed specifically to evaluate the characteristics of films. Noting the similarity of this curve to the Bode plots in circuit theory, we conjecture that the functional form is

$$D = -\log_{10}\left[\frac{(It)^{\gamma} + \beta^{\gamma}}{(It)^{\gamma} + \alpha^{\gamma}}\right]^{\Gamma/\gamma} \qquad (1.2\text{-}1)$$

1.8 H. Frieser and E. Klein, Photographic Science and Engineering 4, 264 (1960).

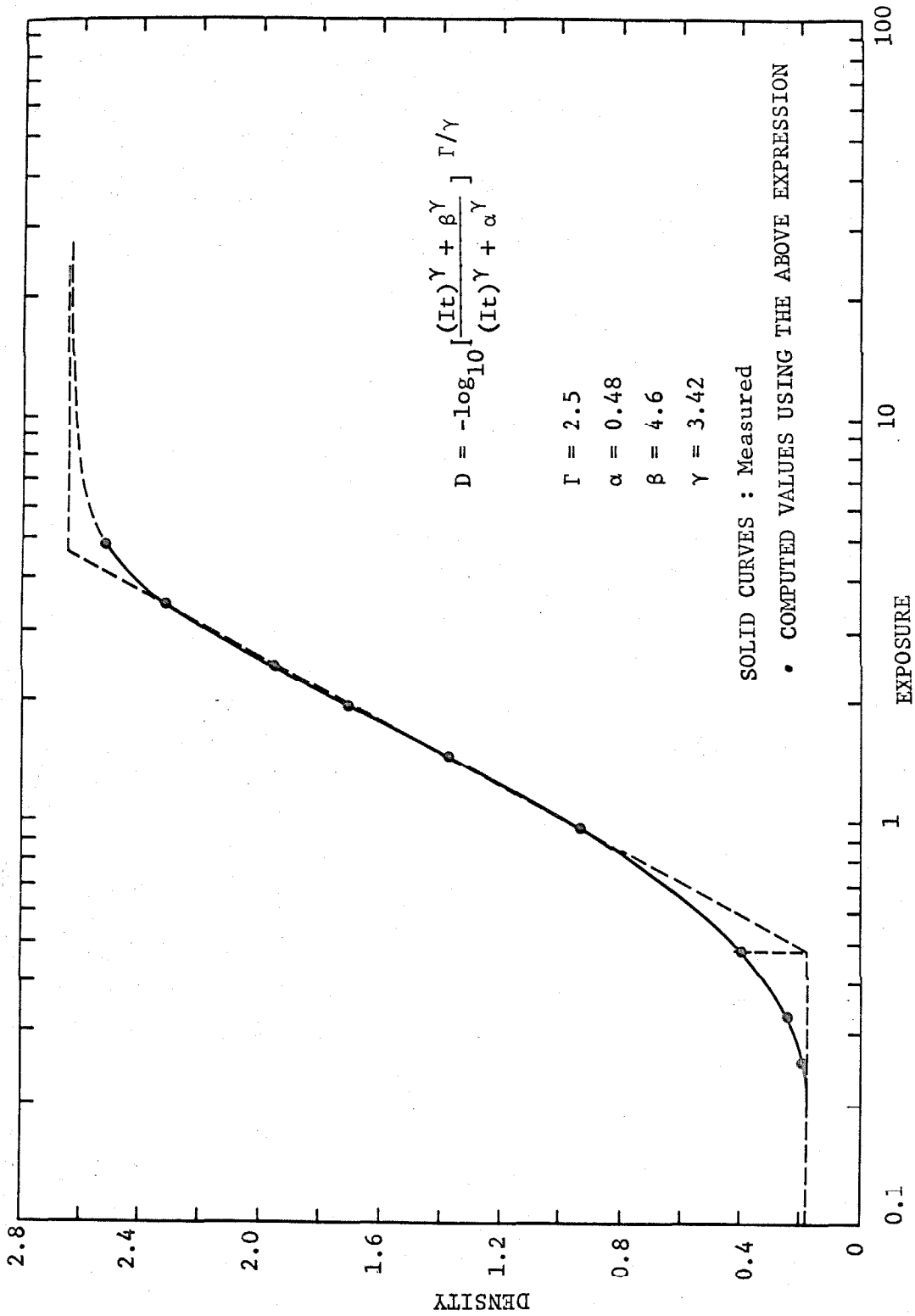

FIGURE 1.2 NUMERICAL CURVE FITTING OF H-D CURVE, 649 F FILM.

where α, β, γ are arbitrary constants to be determined and Γ is the slope of the straight portion of the H-D curve. These three constants can be determined from the values of the maximum density, the minimum density, and the density at the exposure where two of the asymptotes meet. We have determined that for this curve the values of the constants are $\alpha = 0.48$, $\beta = 4.6$, $\gamma = 3.42$ and $\Gamma = 2.50$ and the resulting function is described by the dots in Figure 1.2. We see that the fit is extremely good. We note here that a larger γ (e.g., $\gamma = 4$) gives an even better fit.

1.2.2 Development

After exposure, the film can be developed either by the physical development or the chemical development method. In the physical development method, the silver halide is etched away leaving the silver specks in place. Then the silver ions from the developer (which is generally a solution containing silver nitrate) will aggregate around the silver specks. (This is referred to as the post-fixation physical development.) This development technique has the advantage that the developed silver grains are round. It has the disadvantage that the contrast is low and the fog level is high. In addition, it is difficult to control the reaction. The reason for the desirability of round grains is that they are less lossy due to surface current and cause less scattering noise. The developed silver for the chemical development comes from the grain itself. The mechanism by which silver is formed is similar to that of the formation of the latent image. In this case there is a potential difference between the crystal and the developer (Redox

potential difference) so that the silver speck acts as an electrode. As the silver ion moves towards the silver speck, it is neutralized by the electrons from the developer and tends to push the silver arriving first outward. This causes the developed silver to form into thin long strips.

When developing very thick emulsions (say above 20 microns) caution must be exercised so that the development process is uniform throughout the whole layer. This can be done by soaking the plate in cold developer. Once the plate is thoroughly soaked with the developer the temperature is raised for the development to take place.

It may be of interest to see what is present in a typical developer and see what is the function of each chemical. The most commonly used developer for Kodak 649-F is D-19. The elon and hydroquinone are organic reducers or developers. Sodium sulfite is a weak solvent for silver halide and serves the additional task of a preserver. Sodium carbonate acts as an accelerator and potassium bromide acts as a restrainer. A weak solvent is needed to etch away some crystals and expose the internal specks, a preserver slows down the oxidation of the reducers, and an accelerator increases the pH factor of the developer (more alkaline) thus decreasing the Redox potential of the developer, allowing the silver ion to move faster towards the speck. A restrainer slows down the fogging process by lowering the degree of ionization of the silver bromide by reducing the concentration of the silver ions.

1.2.3 Stop Bath

The stop bath is an acid solution; usually acetic acid. It changes the pH of the surrounding silver halide crystal, which is to say, changes the relative potential difference between the crystal and the developer. This stops the reducing action of the developer. It is found experimentally that an abrupt change of pH may cause the gelatin to shrink or wrinkle, so a quick rinse with water between different solutions is generally considered a good practice.

1.2.4 Fix

Sometimes it is advantageous not to fix the plate, so that the shrinkage is minimized. The cause of shrinkage is discussed in Section 1.2.5.

A fixer generally contains sodium thiosulfate (hypo) which changes the undeveloped silver halide into a silver complex, in this case $Na_3(Ag(S_2O_3)_2)$, which is soluble in water. Hypo does not, in general, react with silver although it has been reported that it reacts with very small silver particles in an acid solution. One must be cautious about the total number of film plates processed in a given fixer bath. This is due to the fact that as the concentration of hypo decreases, it is more likely that the unsoluble complex salt $Na(Ag(S_2O_3))$ will form (1.9). Such formation can be quite detrimental to the image reconstructed from a hologram. This point will become clear after reading the section on bleaches.

1.9 L. Pauling, General Chemistry, 2nd Ed., W. H. Freeman, San Francisco 1953.

1.2.5 Wash

After fixation, the film must be washed in running water so that all the soluble silver complex salts can be dissolved. After this step, the emulsion becomes a suspension of silver particles in a gelatin medium. Small voids exist where the undeveloped grains have been removed, but as the gelatin dries, it collapses into these voids. This, in fact, causes the emulsion to shrink.

1.2.6 Bleaching

It is desirable to change the dark silver grains into dielectric grains with low loss. In Chapter 3 we see that the phase grating is capable of very high diffraction efficiencies. The theory of artificial dielectric will be discussed in Chapter 2. What is required of a bleach is, then, that it must be an oxidizing agent. That is, it must be able to oxidize the silver into a silver salt, which may be substituted later by the salt of a different metal if so desired. We will describe various bleaches that can be used for bleaching holographic plates. Specific remarks on the merit of each bleach, relating to diffraction efficiency will be discussed in Chapter 4 . A few of the bleaches described here can be found in a paper by Upatnieks (1.10).

1.2.6.1. Chromium intensifier. Dissolve 10 grams of potassium dichromate ($K_2Cr_2O_7$) in 1000 cc of water and mix in 18 cc of concentrated hydrochloric acid. The bleaching time is approximately 30 seconds or until clear. The final products in this case are silver chloride and chromic oxide.

1.10 J. Upatnieks and C. Leonard, Appl. Optics 8, 85 (1969).

1.2.6.2. Kodak chromium intensifier. This is a proprietary product and its exact formulation is not known. Dissolve part A and part B as directed. Bleach the fixed film plate in solution A until cleared, rinse it in running water and soak in part B until the yellow stain disappears. Wash the plate with running water for 10 minutes.

This product is more convenient to use than the chromium intensifier because no acid is involved. However, it is found experimentally that if the pre-bleached density is very high, this bleach leaves a reddish-yellow color on the plate which causes scattering noise and loss.

A variation in the use of this bleach is to use part A only. A fairly stable salt; probably silver chromate is formed.

1.2.6.3. Mercuric chloride bleach. Mix 20 grams of mercuric chloride with 1000 cc of water, and add 3 cc of hydrochloric acid. After bleaching,the plate must be rinsed in 1% hydrochloric acid solution and washed thoroughly. A variation of this bleach is substituting the hydrochloric acid with 10 grams of sodium chloride, or 20 grams of potassium bromide, or simply a more concentrated solution of mercuric chloride.

Caution must be exercised when handling HgCl, which is extremely poisonous and may be absorbed by the skin.

1.2.6.4. Potassium ferricyanide cutting reducers. Potassium ferricyanide is a powerful oxidizing agent which will oxidize the silver grains into silver ferrocyanide. This compound can be found in part A of Kadak's Farmer's reducer. The reaction is quite slow and may

take up to 15 minutes.

A modification of this is by mixing 20 grams each of potassium ferricyanide and potassium bromide into 1000 cc of water. This bleach works much faster and produces silver bromide as its end product. If 20 grams of potassium iodide are used instead of the bromide, then the end product is silver iodide.

1.2.7 Reversal Processing

Reversal process in the normal photographic sense means that a positive image is obtained from a negative material. From a holographic point of view, we are merely applying Babinet's theorem in diffraction. The usual procedure is to develop the emulsion without fixing it, so that both the silver grains and silver bromide grains are present. The silver can then be oxidized into a soluble salt, leaving the undeveloped silver bromide grains. For positive slides, the emulsion is redeveloped to form dark images. For holographic work, as mentioned in Section 1.2.6, we prefer dielectric grains; thus the redevelopment step is omitted.

The reversal process has a distinct advantage over the bleaching technique described in previous sections: the grating made this way has very low scattering noise if the correct reversal bath is used. This is reasonable because the grains present at the end for reconstructing the image have not been developed and, as a result, are round, rather than elongated. Electron micrographs of the developed silver and the grains after the reversal process are shown in Figures 1.3 and 1.4. The difference is immediately obvious when

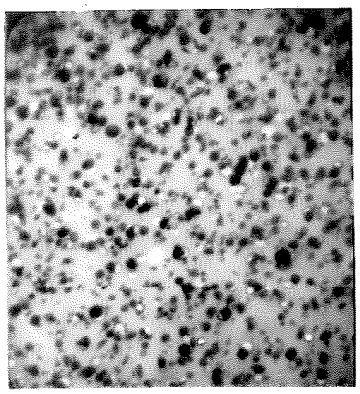

FIGURE 1.3a SILVER HALIDE CRYSTALS IN UNDEVELOPED 10E70

(Magnification $1.68X10^4$)

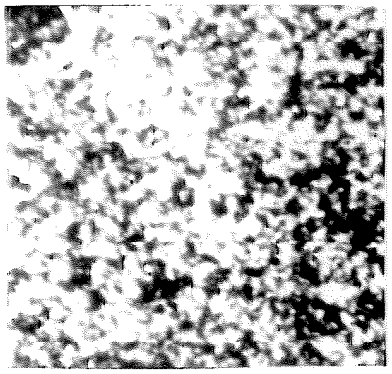

FIGURE 1.3b DEVELOPED SILVER GRAINS IN 10E70

(Magnification $1.68X10^4$)

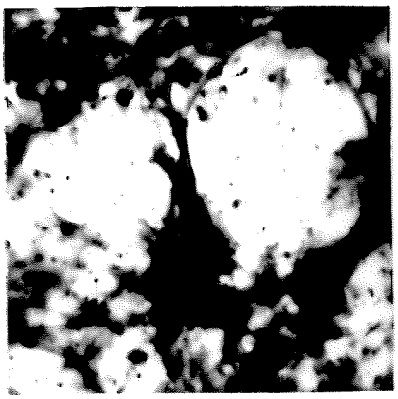

FIGURE 1.3c UNDEVELOPED SILVER HALIDE GRAINS* AFTER HNO_3 REVERSAL BATH IN 10E70

(Magnification $1.68X10^4$)

* The grains are the small dots, the gross structure is the torn gelatin.

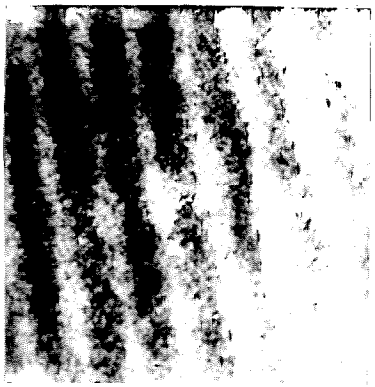

FIGURE 1.4a DEVELOPED SILVER GRAINS IN 649F SHOWING GRATING STRUCTURE

(Magnification $0.31X10^4$)

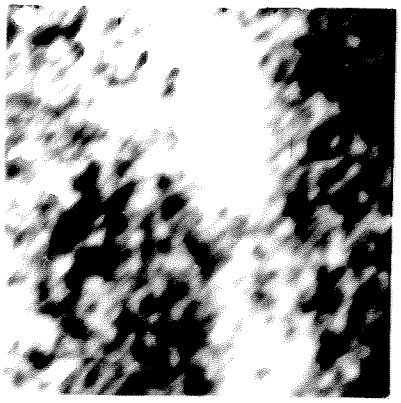

FIGURE 1.4b SAME AS ABOVE

(Magnification $1.68X10^4$)

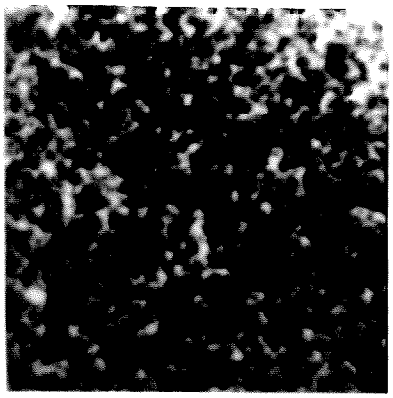

FIGURE 1.4c UNDEVELOPED SILVER HALIDE GRAINS AFTER HNO_3 REVERSAL BATH 649F

(Magnification $1.68X10^4$)

Figure 1.3b and 1.4b are compared with 1.3c and 1.4c, respectively.

Three standard reversal baths are given in Reference (1.3). The cerium sulfate formula given there does not work (the plate remains dark even after prolonged soaking) and is omitted here. We have found a particularly simple way of accomplishing the same task with better results using nitric acid. The process is described below.

1.2.7.1. Permanganate reversal bath. Dissolve 3 grams of potassium permanganate in 1000 cc of water and add 10 cc of concentrated sulphuric acid. This solution reacts with silver to form silver sulfate which is soluble in water. Some brown manganese dioxide is also formed on the emulsion and can be cleared by soaking in a solution containing 10 grams of sodium bisulfite in one liter of water. The plate must be washed thoroughly because the sodium bisulfite solution will sensitize the grains.

1.2.7.2 Dichromate reversal bath. Dissolve 8 grams of potassium dichromate in one liter of water, and add 10 cc of concentrated sulphuric acid. Again silver sulfate is formed and dissolved in water and the plate can be cleared by the sodium bisulfite lye described above.

1.2.7.3. Nitric acid. The unfixed plate is immersed in a shallow basin of water. Pour 1:1 concentrated nitric acid into the water until the plate starts to clear. The plate is taken out when it becomes clear, and is rinsed and dried. The 10E70 emulsion tends to become fragile, but the 649F stands up quite well to this treatment.

Micrographs of gratings produced by different processes are shown in Figures 1.5 through 1.8. The magnification in these micrograph is 500X, and the spatial frequency of these gratings is about 400 lines/mm. The Agfa 10E70 and the Kodak 649F are typical emulsions used for holographic recordings. Figure 1.5 shows the unbleached gratings with a density of approximately 0.5. Figure 1.6 shows gratings that were bleached by the chromium intensifier described in Section 1.2.6.1. The difference in the quality of the two gratings is immediately obvious. The gratings shown in Figure 1.6a has much more scattering noise than 1.6b. We can also see a difference in the quality between those shown in Figures 1.5 and 1.6. This is the reason why it is customary to use unbleached holograms when resolution is more important than the brightness of reconstruction. Figure 1.7 shows the gratings produced by the nitric acid reversal bath. We can see that the quality of these gratings even surpasses that of the unbleached gratings. This is particularly noticeable for gratings produced on the 10E70 plates. Figure 1.8 shows gratings of poor quality resulting from using the other two reversal baths described.

1.2.8 Rinse

After all the processing has been completed, the film plate is immersed in distilled water containing a small amount of Kodak Photo Flo. This reduces the surface tension of the water so that the film will dry smoothly without too much local surface shrinkage. It also causes the water to flow off so that a minimum amount of water mark remains.

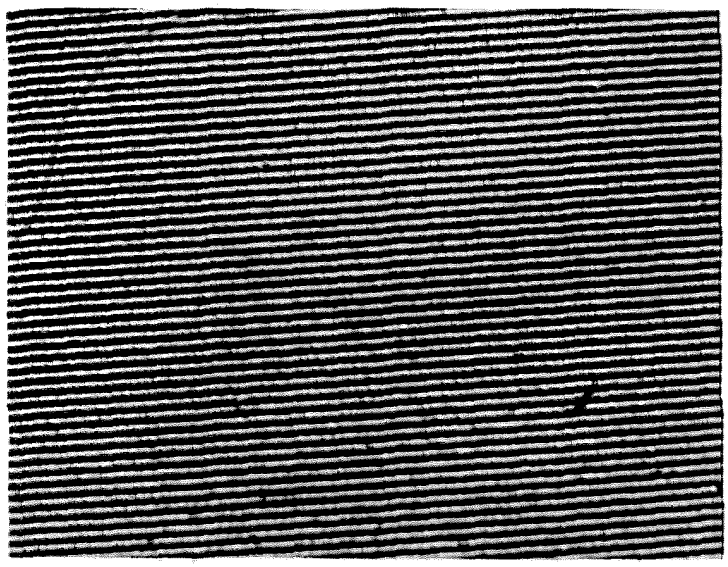

FIGURE 1.5a 10E70 (D-19, 5 MINUTES, 70°F; RAPID FIX) UNBLEACHED.

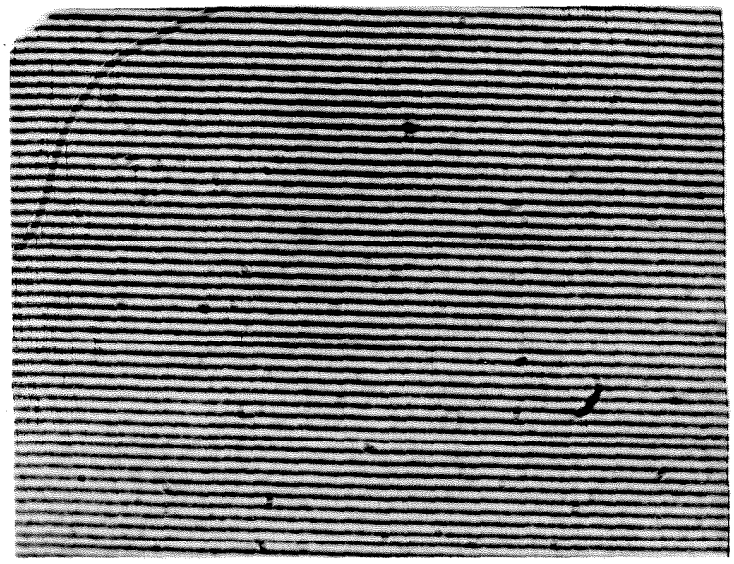

FIGURE 1.5b 649F (D-19, 5 MINUTES, 70°F; RAPID FIX) UNBLEACHED.

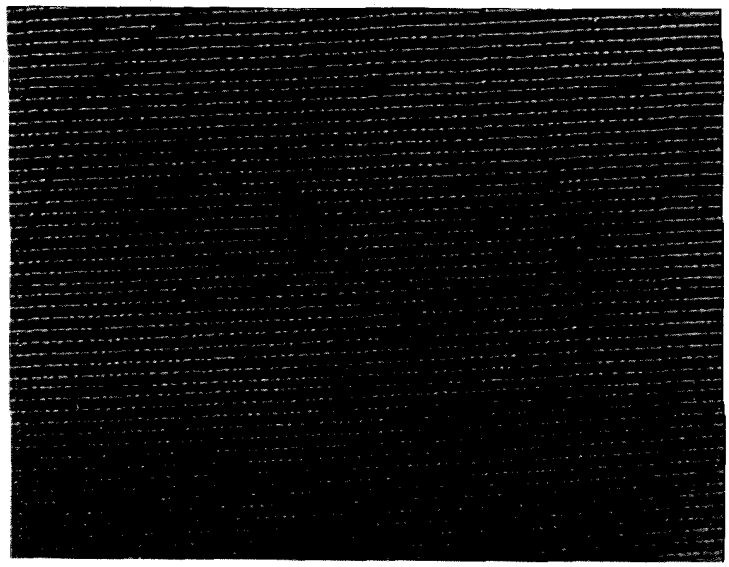

FIGURE 1.6a 10E70 (D-19, 5 MINUTES, 70°F; RAPID FIX) CHROMIUM INTENSIFIER.

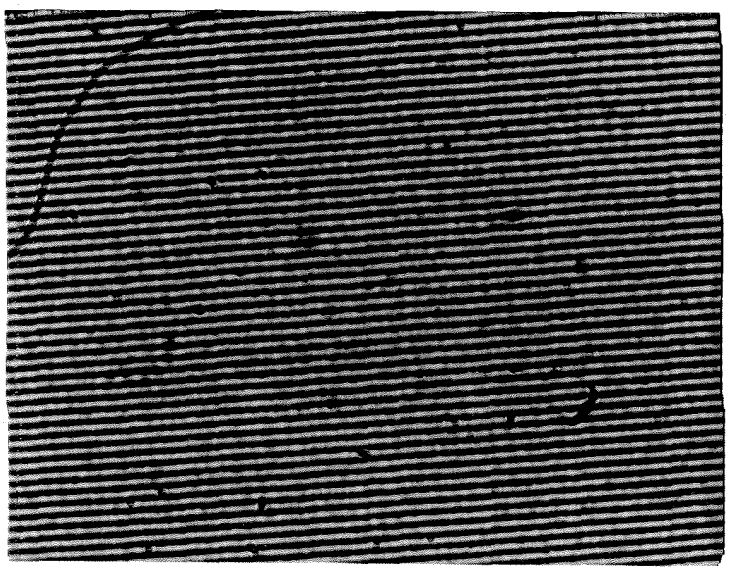

FIGURE 1.6b 649F (D-19, 5 MINUTES, 70°F; RAPID FIX) CHROMIUM INTENSIFIER.

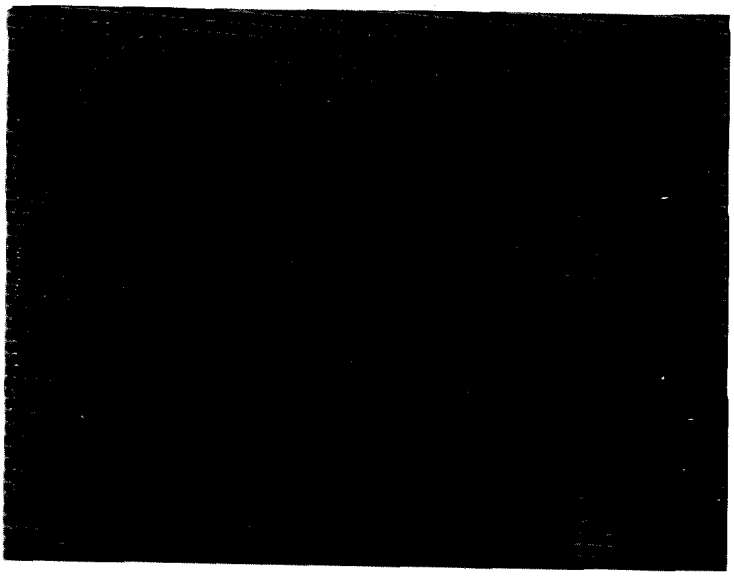

FIGURE 1.7a 10E70 (D-19, 5 MINUTES, 70°F; UNFIXED) HNO_3 REVERSAL BATH.

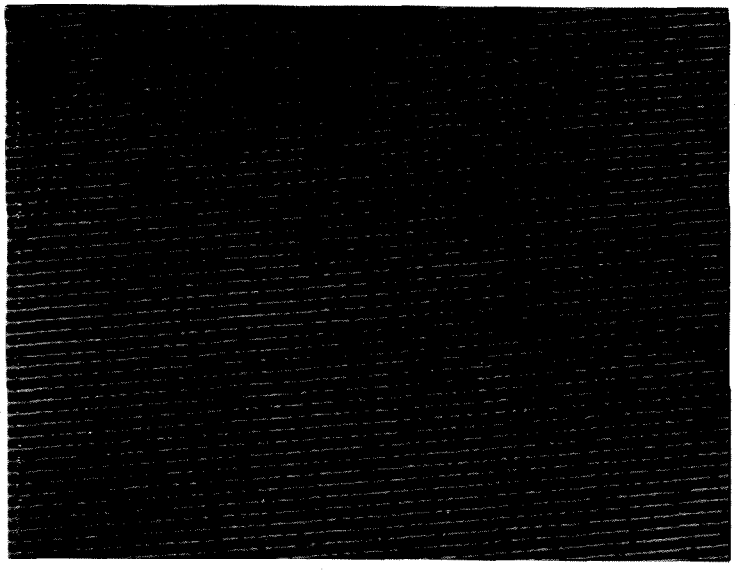

FIGURE 1.7b 649F (D-19, 5 MINUTES, 70°F; UNFIXED) HNO_3 REVERSAL BATH.

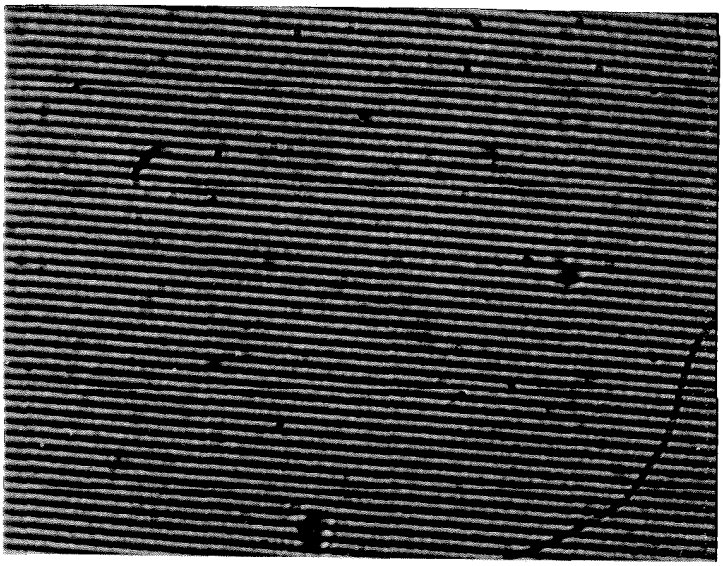

FIGURE 1.8a 649F (D-19, 5 MINUTES, 70°F; UNFIXED) DICHROMATE REVERSAL BATH.

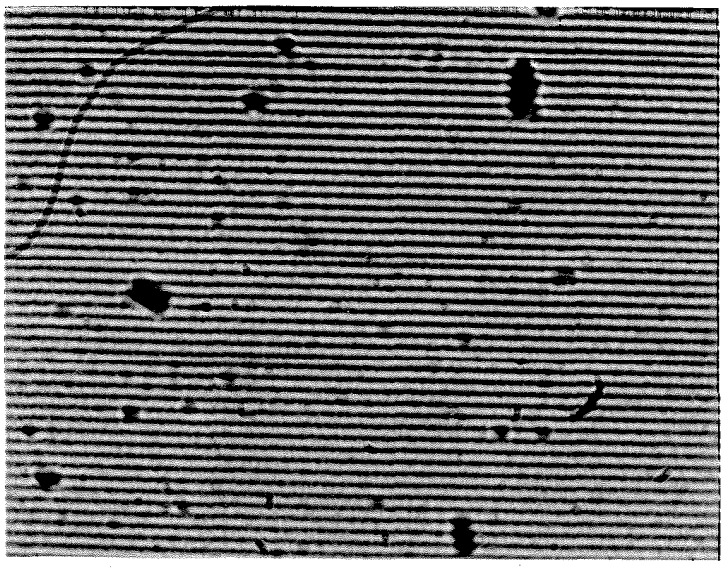

FIGURE 1.8b 649F (D-19, 5 MINUTES, 70°F; UNFIXED) PERMANGANATE REVERSAL BATH.

1.2.9 Swelling of the Emulsion

The processed emulsion tends to shrink, because various salts and constituents in the gelatin has been washed off. It is sometimes necessary to compensate for this loss. Proper swelling is particularly important when we are dealing with reflection type holograms, where the spacing of the grains is important for true color reproduction.

There are several techniques. One method proposed by Lin (1.11) requires soaking the processed emulsion in a 6% triethanolamine water solution for a few minutes. The length of soaking time depends upon the amount of exposure and the process involved. Another method is described by Upatnieks (1.12), which involves soaking the emulsion in Pakosol at twice the normal concentration.

1.2.10 Desensitization

In almost all the bleaches described in the previous sections, the final products are silver salts which are sensitive to light. When exposed to intense light, they will turn black as the salts decompose into silver and their respective by-products that make up the salts. This causes undesirable attenuation of light. It is thus desirable to find some methods to stabilize these

---

1.11 L.H. Lin and C.V. LoBianco, Appl. Optics 6, 1255 (1967)

1.12 J. Upatnieks, Private communication.

salts. Upatnieks (1.10) suggested soaking the processed emulsion in a solution containing their respective cupric halogens (e.g., CuI_2). The motivation for such a procedure is to add an excess of halogen ions in the emulsion, thus reducing the likelihood that the halogen ion formed by splitting off from the silver salt will be absorbed by the constituents of the gelatin. However, the disadvantage of soaking in these solutions is that they tend to crystalize, causing unwanted scattering noise.

In Chapter XLII of Glafkides (1.3) a discussion on desensitization by dye is given. We have soaked plates which have been bleached by the chromium intensifier in a solu n containing 1/2 grams of 147% safranine aconc in one liter of water for 30 seconds, and let dry. We have also soaked the plates in the above mentioned dye solution with 10 grams of sodium sulfite added. In both cases, the plates turned dark at a much slower rate than the untreated plates, although the latter solution seems to work only where the density is low.

1.3 Photochromic material

Photochromism is a property exhibited by certain organic and inorganic compounds, in that, they show reversible color or optical density changes. We will describe two photochromic materials which have been used successfully to make holograms. They are photochromic glass and alkali halide single crystals. Their properties and the physical mechanisms involved in each process will be briefly described below. Certain photochromic sodalite films that are available commercially will not be described here because they are thin, incapable

of reaching density higher than unity and are subject to fatigue.

1.3.1 Photochromic Glass

Photochromic glass is borosilicate glass containing silver halide crystals (1.13) of approximately 50 to 100Å in size and spaced 500 to 1000Å apart. The physical mechanism involved is very similar to that of the photographic emulsions. The difference is that in this case the host material, glass, is nonpermeable to the halide atoms, so that they are available for recombination with the silver as soon as the exposing field is removed. This is called thermal fading and can be slowed down considerably by cooling. In addition, since the grains cannot effectively use sensitizers in their host medium, they are only able to absorb in the blue and near the ultraviolet region of the spectrum. Furthermore, the quantum gain is less than one because no development is involved. Visible light between 5500-6500Å can also be used to bleach the darkened plate. The mechanisms involved here are not well understood, and it is surmised that photo-ionization takes place which accelerates the recombination of the silver and the bromide. Thermal fading cannot be optimally used for data storage, but selective bleaching can be used to cause amplitude transmittance variations for light diffraction.

Generally, the plate is first darkened with an ultraviolet source, such as a xenon arc lamp, to a density of .8 for a 5 mm thick sample. It can then be exposed with any laser in the visible range. In most cases, the laser light is not intense enough to bleach the

---

1.13 G. K. Megla, Appl. Optics 5, 945 (1966).

plate fast enough for the thermal fading to be negligible. It is then desirable to shine the UV light on the glass plate while bleaching takes place. Once the hologram is stored, the plate has to be cooled to retain the image.

One definite drawback in using photochromic glass is its speed. We see that the quantum yield is less than one, so that we expect the sensitivity of this material to be about six to eight orders of magnitude slower than that of photographic film for reaching the same density. (Typical material with special sensitizers is about four orders of magnitude slower than the 649F plates). Thermal fading time can vary from a few minutes to a few weeks depending upon the type of material chosen. Thermal fading makes this material somewhat unsuitable for long term data storage, but can be used adequately for real-time systems. The gamma, slope of the density versus logarithm of exposure curve, is low and is typically less than one. This makes it unattractive for applications in image restoration, match filtering and optical data processing. In most cases, a gamma greater than unity is desirable. The resolution of this material is high; holographic gratings of spatial frequency 2000 lines/mm have been successfully recorded.

1.3.2 Alkali Halide Crystals

Alkali halide crystals with appropriate impurities are available commercially for holographic use. One such crystal is potassium bromide with potassium hydride and is described on page 149 of

Reference (1.5). Potassium hydride (KH) is incorporated into KBr during the formation of the crystal, and the H^- ion takes the position of a normal Br^- ion. This gives rise to a new absorption band in the ultraviolet, called the U-band. When a photon in the UV is absorbed, it lifts an electron into a free state, changing the hydrogen ion into a neutral atom. The neutral hydrogen atom can diffuse away leaving a vacancy for the electron. An electron taking the place of a negative ion is called an F-center and has absorption characteristics determined by the crystal structure. For potassium bromide crystal the absorption band for the F-center is in the red and the crystal appears blue. When a photon in the absorption band of the F-center is absorbed, it may free an electron from an F-center and the reverse process may take place.

In using such crystal for holographic recording, it is first irradiated with ultraviolet light until it turns blue. It is then bleached with laser light. This bleaching or ionization process is highly temperature dependent. A standard procedure to speed up the bleaching process is heating the crystal to 80°C.

There are several disadvantages in using this crystal. It has an extremely low sensitivity, about two to three orders of magnitude lower than that of the 649-F at 6328Å. During the writing period, heating is quite undesirable as the interference pattern becomes unstable due to the hot turbulent air. This disadvantage may be overcome by placing the whole holographic setup in a vacuum chamber.

We have produced holographic gratings of approximately 1500 lines/mm without special precautionary measures and have obtained an

efficiency of less than one percent.

1.4 Photoresist

Photoresist is a formulation of liquid resins which is sensitive to light in the ultraviolet spectrum. The resist polymerizes when exposed and may be selectively dissolved by a "developer". One such developer is the trichloroethylene. Sheridon (1.14) has found that gratings with efficiency up to 73% can be produced this way. It has also been found that a small change in the index of refraction takes place due to polymerization. Maurer (1.15) found that an index change of .01 is possible in an undeveloped photoresist and has made gratings with an efficiency of 60%.

1.5 Thermoplastics

Thermoplastic can be used for holography by applying the technique of xerograph. The thermoplastic is first coated on a photoconducting substrate. It is then charged on both sides with opposite electric charges in the absence of light. When it is exposed to light, the charge at the exposed portion are able to move closer towards each other through the photoconducting substrate such that a higher static potential exists there. If the plate is now heated, different static potentials will cause different amounts of deformation as the plastic becomes softened. Urback (1.16) has demonstrated the possibility of holographic recording with such material and holograms of reasonable quality have been produced.

1.14 N.K. Sheridon, Appl. Phys. Letters 12, 316 (1968).

1.15 D.W. Maurer and E.E. Francois, IEEE Conf.on Laser Engineering and applications, Washington, D.C. (1967).

1.6 Photosensitive Plastics

Certain thermal plastic resin coatings that contain light sensitive diazonium salt also seem to be applicable for low spatial recordings. One such film utilizes the Kalvar process (1.17). The diazonium salt is sensitive to ultraviolet light and releases nitrogen during exposure. By heating the sample, the air bubble is made to expand and form microscopic vesicules which have an index of refraction close to unity. The difference in the index of refraction, as shown in the next chapter, can cause the index modulation needed for holographic process. After cooling off, the plate can be exposed to light and the image is permanent if all the diazonium salt decomposes and the nitrogen diffuses away before it is subjected to heating.

Such film has not been used in holography thus far because a good laser operating in the 3000 Å range is not available and the film is only suitable for low spatial frequency recording since it has a resolution of only 500 lines/mm.

1.7 Ferroelectric Crystals

Single crystal lithium noibate ($LiNbO_3$) has also been used to record holograms. When exposed to light of short wavelengths, photoexcitation frees the trapped charges which can drift a short distance before becoming retrapped. The field created by the space charges

---

1.16 J.C. Urback and R.W. Meier, Appl. Opt. 5, 666 (1966).

1.17 W. A. Siefert and W. F. Elbrecht, Photographic Science and Engineering 5, 235 (1961).

causes changes in the refractive indices due to electro-optical effects. Chen (1.18) has made diffraction gratings with 1600 lines/mm and obtained 40% efficiency. It is observed that the recording has a finite life time and may be erased by heating. This material has the potential of becoming a very important medium for optical data storage.

1.8 Dichromated Gelatin

It has long been known that when gelatin is treated with water soluble dichromates and chromates, the gelatin becomes hardened and less soluble in water. Recently, Shankoff (1.19) has demonstrated that highly efficient gratings with good resolving power can be produced on dichromated gelatin. Efficiency of 95% has been observed and the speed is comparable to that of 649F in the blue region of the spectrum. Development consists of agitating in water for 30 seconds and dipping in isopropanol for fast drying. It is perhaps due to this fast drying that resolution of 4000 lines/mm was observed. The structure of the developed gelatin is still uncertain, but it is safe to say that much of the diffraction is due to surface effect, which makes it somewhat less suitable for high density data storage than some of the materials described above which involve internal index modulation.

1.9 Photopolymer

A photopolymer system contains a monomer, a catalyst, a photo-oxidant and a fixing agent has recently been used to record holograms (1.20). In this system the photo-oxidant is activated by

---

1.18 F.S. Chen, et al., Appl. Phys. Letters 13, 223 (1968).

1.19 T. A. Shankoff and R. K. Curran, Appl. Phys. Letters 13, 239 (1968).

1.20 D. H. Close, et al., Appl. Phys. Letters, to be published; "Hughes Photopolymer System", Hughes Aircraft Co. TM-871 (1966).

the photons absorbed so that it oxidizes the catalyst. The catalyst in turn initiates free-radical polymerization. Fixing can be done by heating or by exposing the system to ultraviolet light which deactivates the oxidant. Stable holograms has been recorded and gratings of approximately 1000 lines per millimeter with efficiency of 45% has been obtained. The disadvantage of such a system is that it is found to be noisy, which is due to scattering by long polymer chains.

CHAPTER TWO

DIELECTRIC CONSTANTS OF PHOTOGRAPHIC EMULSIONS

2.1 Introduction

Developed photographic emulsion is made up of a random suspension of silver particles in a gelatin medium. Following the bleaching process described in Chapter One, the silver particles are changed into dielectric grains. Electron micrographs of typical emulsions developed in D-19 show that the grains are not round, but are elongated and are approximately 500Å in length(see Figures 1.3 and 1.4).

The purpose of this chapter is two fold. It makes possible the correct formulation of the index of refraction which is essential for calculating the diffraction efficiency when loss is included in the analysis. The effective index of refraction of the emulsion, composed of gelatin and the grains, each with a different index of refraction, is analysed as an artificial or loaded dielectric in this chapter. The other purpose of this chapter is to establish the relationships of many factors between the bleached emulsions and their unbleached counterparts. We have related the effective dielectric constant of a bleached emulsion to the pre-bleached density and the modulation transfer function (MTF) before and after bleaching. This is a necessary step because both the MTF and the effective dielectric constant of a bleached emulsion are difficult to measure, whereas the MTF and the density of unbleached emulsions can be measured with automated equipment. The importance of this analysis can be illustrated with an example. If we expose the emulsion with a sinusoidally modulated intensity as shown in Figure 2.1

to obtain a sinusoidally modulated index of refraction, we need an emulsion which has a linear curve of the index of refraction change versus exposure. In practice, it is almost impossible to obtain this curve, particularly at low exposure. However, from the analysis to be given in this chapter, we can specify the required density-exposure curve instead which can be easily obtained for all emulsions by replotting their H-D curves. Another result of some importance is that we have shown analytically that the MTF can be improved to unity for a given spatial frequency. This opens the possibility of producing gratings with extremely small line spacings which could not otherwise be produced even at a great expense.

2.2 Effective Dielectric Constant

The theory of artificial dielectric material was under intensive study in the development of microwave lenses. Noteworthy is the work of Lewin (2.1).The scattered field of a single grain is first derived and the field contributed by neighboring grains is either compensated by adding all the scattered fields or by applying the Clausius-Mossotti relation (sometimes referred to as Lorentz-Lorenz formula) (2.2). In this analysis we will consider that each grain is spherical and is much smaller than the wavelength.

The polarizability of a grain much smaller than a wavelength based on the scattered field using Mie's theory(2.2), is given by $a^3\varepsilon_1(\varepsilon_2 - \varepsilon_1)/(\varepsilon_2 + 2\varepsilon_1)$ where a is the radius of the sphere, ε_1 and

---

2.1 L. Lewin, J.I.E.E. 94, 65 (1947), Part 3.

2.2 M. Born and E. Wolf, Principles of Optics, 3rd Edition, Pergamon Press, Oxford (1965)

ε_2 are the dielectric constant of the medium and the scatterer, respectively. Applying the Lorentz-Lorenz formula

$$\varepsilon/\varepsilon_1 = (1 + \frac{8\pi}{3} N\alpha) \; / \; (1 - \frac{4\pi}{3} N\alpha)$$

where α is the polarizability, N is the number of grains per unit volume, one obtains the following expression for the effective dielectric constant ε :

$$\varepsilon = n^2 = \varepsilon_1 \{1 + 3f/[(\varepsilon_2 + 2\varepsilon_1)/(\varepsilon_2 - \varepsilon_1) - f]\} \qquad (2.2\text{-}1)$$

where $f = N \frac{4}{3} \pi a^3$.

f is called the filling factor, which is the volume of scatterer per unit volume of the medium. We are only interested in $(\varepsilon - \varepsilon_1)$, the effective index change. By examining the tabulated results of the effective dielectric constants of scatterers with common geometric shapes, it is concluded that our results are correct to within a multiplicative constant (2.3) by assuming the grains to be spherical.

In the case of silver $\varepsilon_2 = \varepsilon'_2 + i\varepsilon''_2$ where ε'_2 and ε''_2 are the real and imaginary parts of ε_2 . For this analysis, we have assumed that ε_2 remains fixed over the entire range of densities encountered for a given emulsion. For $f \ll 1$, equation 2.2-1 can be

---

2.3 S. B. Cohn, Proc. of Symposium on Modern Advances in Microwave Techniques, Polytechnic Press, N.Y. (1954), p. 465.

simplified to

$$n = n_1\{1 + 1.5f(\varepsilon_2'^2 + \varepsilon_2''^2 - 2\varepsilon_1^2 + \varepsilon_1\varepsilon_2')/[(\varepsilon_2' + 2\varepsilon_1)^2 + \varepsilon_2''^2]\}$$

$$+ i\{4.5\ fn_1\varepsilon_1\varepsilon_2''/[(\varepsilon_2' + 2\varepsilon_1)^2 + \varepsilon_2''^2]\}$$

$$= n' + ifn'' \qquad (2.2\text{-}2)$$

Therefore, for a given thickness L and wavelength λ, the density D is given by

$$D = .4343\ fn''(2\pi L/\lambda) \qquad (2.2\text{-}3)$$

The values of ε_2' and ε_2'' depend on how loosely the silver grains are packed and are related to the "covering power" (1.2) of a given emulsion.

Using ε_3 to denote the dielectric constant of the grain after bleaching, (again assume f to be small) equation 2.2-1 becomes

$$n = n_1\left[1 + 1.5\ f'\ \frac{\varepsilon_3 - \varepsilon_1}{\varepsilon_3 + 2\varepsilon_1}\right]$$

$$= n_1 + f'\ \Delta n \qquad (2.2\text{-}4)$$

where $\Delta n = 1.5\ n_1\ \dfrac{\varepsilon_3 - \varepsilon_1}{\varepsilon_3 + 2\varepsilon_1}$

f' is related to f by

$$f' = \left(\frac{\text{Molecular volume of dielectric}}{\text{Molecular volume of silver}}\right) f = \zeta f \qquad (2.2\text{-}5)$$

where we call ζ the expansion factor. Equation 2.2-5 must be modified accordingly if during the bleaching process some of the silver salt is dissolved.

For an emulsion with $D = \beta It$, where β is a proportionality constant, I is the intensity of the light exposing the film, and t is the total exposure time (we have neglected the reciprocity failure effect here), that is, an emulsion with linear density versus exposure curve; then we obtain

$$f = \beta It\lambda / (.8686\ \pi Ln'') \qquad (2.2\text{-}6)$$

This equation can now be used in equation 2.2-4 to find the effective index change after exposure (Or between portions of the film with different exposure).

$$n - n_1 = n_1 \zeta \beta It\lambda\ \Delta n / (.8686 \pi Ln'' n_1) \qquad (2.2\text{-}7)$$

Equation 2.2-7 shows that for an emulsion with $D = \beta It$, the index change is linearly proportional to the exposure.

In making holographic spatial filters, it is generally desirable to have a material that has a linear amplitude transmittance versus exposure curve; this point has been emphasized by many authors (2.4). We note that in arriving at this result, the Kirchhoff diffraction formula has been used, which implies that the film is so thin that only the transmittance on a surface need to be considered. Therefore in

---

2.4 A. Kozma, J. Opt. Soc. Am. 56, 428 (1966).

comparing their result with the condition $D = \beta It$ given above, we have to show that the two are equivalent when the film becomes sufficiently thin. The amplitude transmittance is given by

$$T_{amp} = e^{-AL/2} = 10^{-D/2} \qquad (2.2\text{-}8)$$

where A is the "absorbency" of the emulsion per unit thickness, and L is the thickness. For small AL, the exponential can be expanded,

$$T_{amp} = 1 - AL/2 \qquad (2.2\text{-}9)$$

but from equation 2.2-8 we see that $D = AL \log_{10} e = .4343\ AL$, therefore

$$T_{amp} = 1 - D/.8686$$

$$= 1 - \beta It/.8686 \qquad (2.2\text{-}10)$$

which indeed has the linear dependence to the exposure as cited in the literature.

In the case of making a grating, the film plate is exposed to two plane waves as shown in Figure 2.1. The intensity of the exposure is given by $I_o[1 + \cos(Kx)]$, where $K = 4\pi \sin\theta/\lambda$ and is often referred to as the spatial frequency. The index of refraction after exposure and processing is given by

$$n = n_1[1 + \beta\zeta\ I_o t(1 + \cos Kx)\lambda\ \Delta n/\ (.8686\pi\ Ln"n_1)]$$

$$= n_1 + \eta(1 + \cos Kx) \qquad (2.2\text{-}11)$$

or

$$\varepsilon \simeq \varepsilon_1 + 2n_1\eta(1 + \cos Kx) \qquad \text{for small } \eta \qquad (2.2\text{-}12)$$

where we define

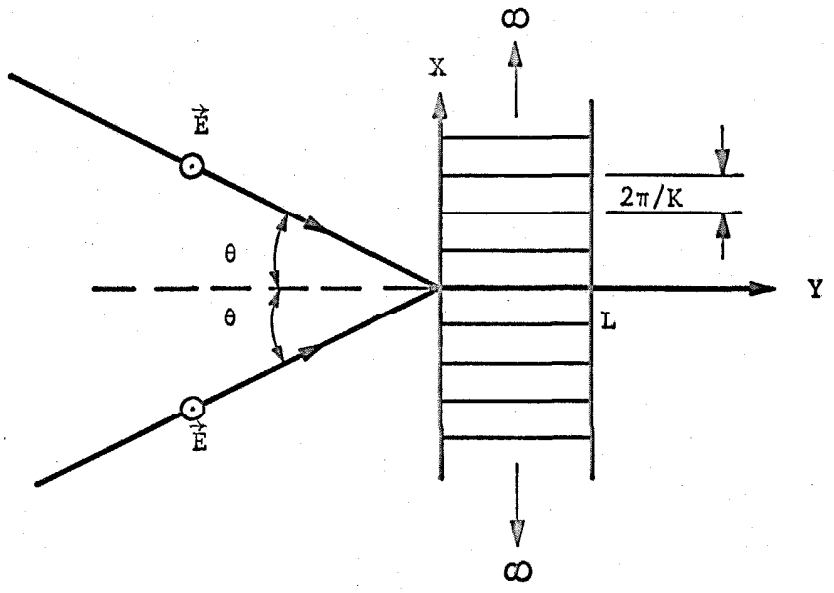

FIGURE 2.1a RECORDING OF HOLOGRAPHIC GRATING

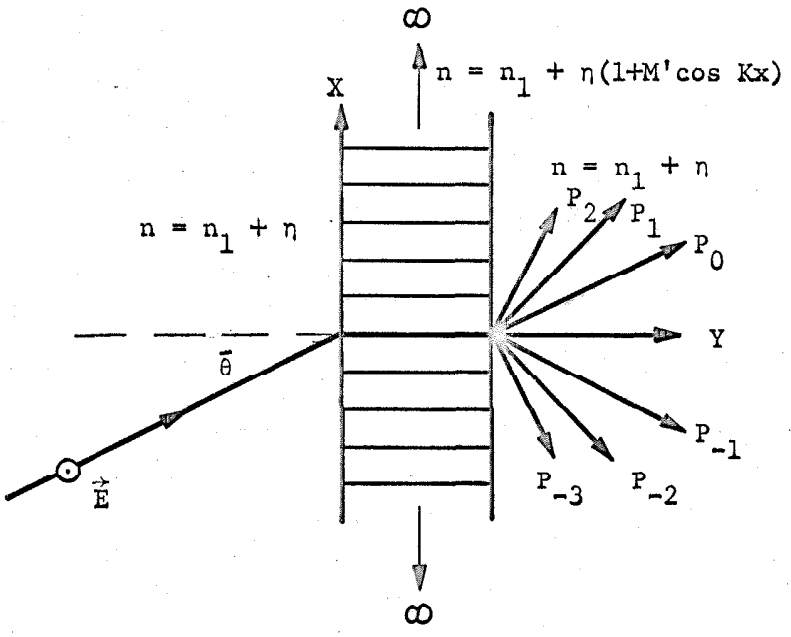

FIGURE 2.1b DIFFRACTION OF LIGHT BY GRATING

$$\eta = \beta\zeta I_o t\lambda \, \Delta n/(.8686 \, \pi Ln'') = f'\Delta n$$

From Chapter One we see that the dielectric grains are generally lossy. The small index change due to the presence of grains may be expressed in the complex form $\eta = \eta' + i\eta''$. It can be substituted into 2.2-11 and 2.2-12 directly.

We note that the sinusoidal modulation of the index of refraction as given in 2.2-12 is made possible only because the emulsion has the $D = \beta It$ response.

We further note that different exposure merely changes the values of η' and η'' but not their ratio. This ratio is determined by the factor Δn as defined in equation 2.2-4.

2.3 The Modulation Transfer Function (MTF)

The modulation transfer function of an emulsion describes how well the film records different spatial frequencies. An analogy can be drawn to the frequency response of an amplifier near the cutoff frequency. The emulsion is exposed with a sinusoidal pattern of the form $(1 + \cos Kx)$; and the MTF is defined as (1.2)

$$M = \frac{T_{max} - T_{min}}{T_{max} + T_{min}} \qquad (2.3\text{-}1)$$

where T_{max} and T_{min} are the maximum and minimum intensity transmittance of the film after development. In other words, the exposed film has an intensity transmittance given by $T = (1 + M \cos Kx)$ where K is the spatial frequency of the pattern used. For the case of bleached plates, the MTF has not been well defined, and it seems reasonable to do

so in terms of the ratio of the amount of index modulation to the total index change as a function of the spatial frequency. That is, for each spatial frequency the film plate should be exposed to the same illuminating intensity. The phase shift can then be measured by an interference microscope. Such measurement has been carried out by Hannes (2.5).

Using the definition of density $D = \log_{10}(1/T)$ and equation 2.2-3

$$D = \log_{10}(1/(1+M \cos Kx)) = .8686\pi\, Lfn''/\lambda \qquad (2.3\text{-}2)$$

f may be expressed in terms of D and is really dependent on the position x, neglecting diffraction effects. Substituting f into equation 2.2-4 and using 2.3-2, one obtains

$$n = n_1 - \Delta n\zeta\lambda/(.8686\pi\, Ln'')\log_{10}(1+M \cos Kx)$$

The net index change, the difference between the largest value of index and lowest value of index, is

$$\delta n = n - n_1$$

$$= - \Delta n\zeta\lambda/(.8686\pi\, Ln'')\, \log_{10}[(1+M)/(1-M)] \qquad (2.3\text{-}3)$$

At first glance equation 2.3-3 has a singularity at $M = 1$; here we will show that M is always smaller than unity.

$$M = (T_{max} - T_{min})/(T_{max} + T_{min})$$

2.5 H. Hannes, J. Opt. Soc. Am. 58, 140 (1968).

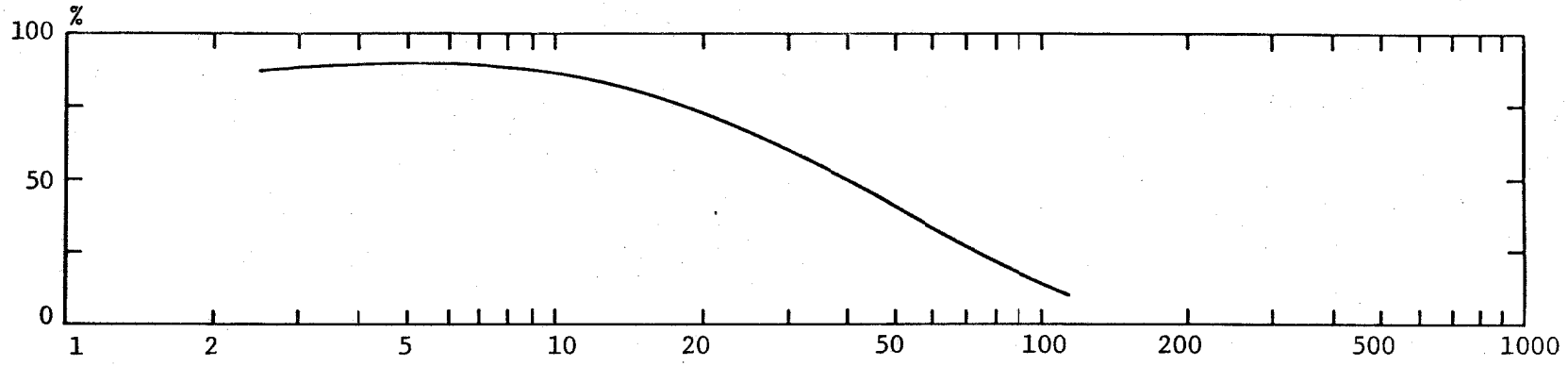

FIGURE 2.2a THE MODULATION TRANSFER FUNCTION OF KODAK HIGH CONTRAST COPY FILM. % MODULATION OF TRANSMITTANCE VERSUS SPATIAL FREQUENCIES IN LINES /mm.

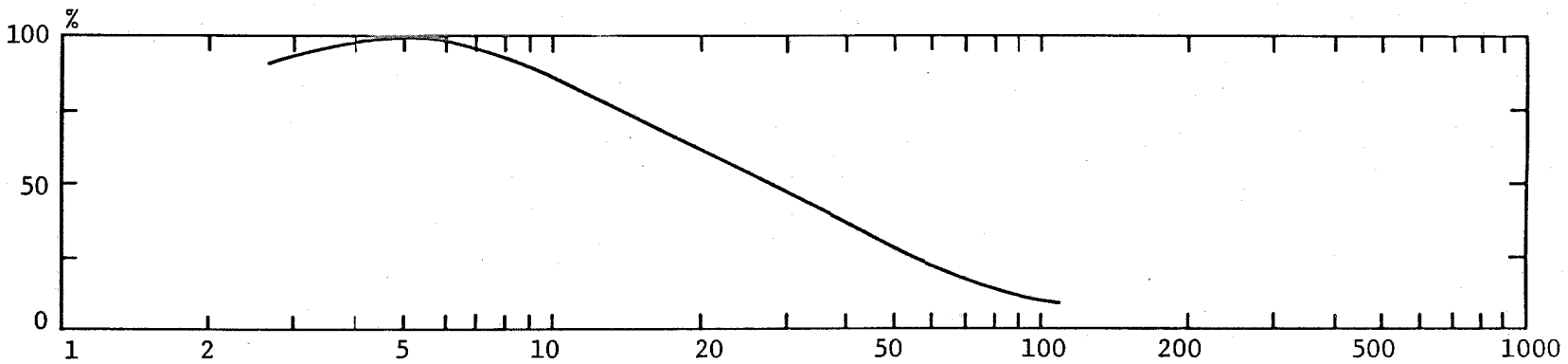

FIGURE 2.2b THE CORRESPONDING MODULATION OF INDEX OF REFRACTION AFTER THE ABOVE FILM HAS BEEN BLEACHED. % MODULATION OF INDEX OF REFRACTION (NORMALIZED TO VALUE AT 5 LINES/mm) VERSUS SPATIAL FREQUENCIES IN LINES /mm.

therefore

$$M_{max} = (1 - T_{min})/(1 + T_{min}) \simeq 1 - 2\,T_{min} \qquad (2.3\text{-}4)$$

Consequently, the maximum value of the factor $\log_{10}[(1+M)/(1-M)]$ is given by $\log_{10}(1/T_{min} - 1) \simeq D_{max}$. Most of the published data on the MTF of films actually has M greater than unity. The reason for this is because M has been normalized to its value at zero spatial frequency.

By using the definition of D given in 2.3-2 we obtain from 2.3-3 that $\delta n_{max} = f'\Delta n$, which implies a modulation of unity.

Equation 2.3-3 shows that if we know the modulation transfer function of a film, we can calculate the effective index modulation after bleaching. Furthermore equations 2.2-11 and 2.2-12 must be modified to

$$n = n_1 + \eta(1 + \frac{\delta n}{\Delta n f'} \cos Kx) = n_1 + \eta(1 + M' \cos Kx) \qquad (2.3\text{-}5)$$

$$\varepsilon = \varepsilon_1 + 2n_1\eta\,(1 + \frac{\delta n}{\Delta n f'} \cos Kx) = \varepsilon_1 + \Delta\varepsilon\,(1 + M' \cos Kx) \qquad (2.3\text{-}6)$$

Hannes has measured the index modulation of the Agfa AgePan FF film as a function of spatial frequency. Unfortunately the modulation transfer function of this film is not available to us. In Figure 2.2 the modulation transfer function of a similar film, Kodak high contrast copy (2.6) , is presented. The factor $\mathrm{Log}_{10}[(1+M)/(1-M)]$ for each M is also calculated and plotted in the same figure. It is expected that M' drops off faster than the above factor at higher spatial frequencies because molecular cross-linking of silver complexes probably takes

---

2.6 Kodak Pamphlet #P49, "Modulation Transfer Data for Kodak Films", Eastman Kodak Company, Rochester, New York (1967).

place during the bleaching process, which effectively decreases M'.

Let us examine Figure 1.4 more closely, paying special attention to the grating structure shown in the first electron micrograph. We can see immediately the reason for M to be less than one. This is due to the presence of grains in regions where there is no exposure. In the next section, a method of increasing the MTF of a dielectric grating is proposed.

2.3.1 Improvement of the MTF

An improvement of the MTF of a film is of great interest. In the discussion here, we are not improving the MTF in the sense of improving the resolution of the film material. If the MTF is zero at a certain spatial frequency, then the method of compensation described below will not help. This method only improves the modulation if the recording already exists.

It is obvious then by examining the electron micrograph, that one method of increasing the MTF is to dissolve the grains where they are not wanted. We can write equation 2.2-11 in the form

$$n = n_1 + \eta(1 - M') + \eta M'(1 + \cos Kx) \qquad (2.3\text{-}7)$$

If we uniformly subtract an exact amount of grains that contributes the small index change $\eta(1 - M')$, we have effectively increase the modulation to unity ! By examining equation 2.3-7 we note that the amount of subtraction depends upon M' which is a function of the spatial frequency. This equation can serve as an analytic basis that the resolution can be increased if indeed such a chemical solution,which subtracts the number of grains uniformly, can be found.

It has long been known that superproportional reducers and certain intensifiers can be used to increase the resolution of films (2.7). The superproportional reducers tend to attack the individual grains more than an aggregate of grains. This tendency suggests the possibility of improving the index modulation over a range of spatial frequencies which can then be applied to producing better holograms when the object subtends a small angle from the plate.

2.7 F.D. Perrin and J.H. Altman, JOSA 42 462, (1952).

CHAPTER THREE

THEORY OF DIELECTRIC DIFFRACTION GRATINGS

3.1 Introduction

A diffraction grating is an optical element that changes the amplitude and phase of an incident wave in a periodic manner. There are two main types of diffraction gratings, the transmission type and the reflection type. In this chapter we will deal only with gratings of the transmission type. The term"dielectric gratings"has been widely applied to gratings which are produced holographically, i.e., the interference pattern of two monochromatic plane waves is recorded in a medium, such as a photographic emulsion, so that a periodic variation of amplitude transmittance or index of refraction results. Our main interest in studying such a grating is to gain some insight into the process of image reconstruction in holography, which is a more general form of grating. A comprehensive treatise on the subject of holography can be found in the thesis report of Matthews (3.1). His analysis treats holography as a recording of the interference pattern of an infinite set of plane waves with different amplitudes and directions. The results obtained here perhaps even go beyond merely academic interest. Better holographic materials and more powerful lasers are now available, so that large gratings of excellent quality can be produced commercially and in the more general forms of gratings can replace conventional optical elements.

3.1 J. W. Matthews, "Theory of Holography", Sc. Report No. 7, Quantum Electronics Laboratory, California Institute of Technology, Pasadena, California 1967.

The basis of this treatment is similar to the generalized theory of Raman and Nath on the diffraction of light by ultrasound (3.2). Starting with the Maxwell's equations, a difference differential equation is derived. An exact formal solution using Laplace transformation, as well as approximate solutions for specific parameters are obtained. The conditions restricting their applicability are precisely stated. Loss is also included in this analysis which may be useful for many practical situations.

A computer solution of the difference differential equation, using the parameters which we encountered in holographic gratings produced on photographic emulsion, is presented. And we have established the maximum obtainable efficiency for a substrate with a fixed thickness.

3.2 Generalized Raman-Nath Theory

A series of papers were published by Raman and Nath to explain the diffraction phenomena observed when light propagates through an ultrasonic column. In the first two papers, they assumed that a plane wave propagating through the grating has no amplitude change, but emerges with phase modulation. The output wave is then decomposed into a spectrum of plane waves. This theory is later modified to include both phase and amplitude change as the wave propagates through the medium. This is often referred to as the generalized theory. An

---

3.2 C.V. Raman and N. S. N. Nath, Proc. Ind. Acad. Sci. A 2,406,413 (1935); ibid., 3, 75, 119 (1936); also N. S. N. Nath, Proc. Ind. Acad. Sci. A 4 (1936); ibid., A, 8, 499 (1938)

excellent summary of their derivation is given by Born and Wolf (2.2) and is included here with some modification for completeness. A very comprehensive survey of the theory of ultrasonic diffraction theory up to 1964 can be found in a report by Gill (3.3) and in a recent book by Berry (3.4). Another useful reference is a paper entitled "Unified approach to ultrasonic light diffraction" by Klein and Cook (3.5).

Maxwell's equations and their constitutive relations in a source-free, non-magnetic medium can be written as:

$$\text{curl } \vec{E} = -\frac{1}{c}\frac{\partial \vec{H}}{\partial t} \qquad \text{curl } \vec{H} = \frac{1}{c}\frac{\partial \vec{D}}{\partial t}$$

$$\text{div } \vec{H} = 0 \qquad \text{div } \vec{D} = 0$$

$$\vec{D} = \varepsilon \vec{E} \tag{3.2-1}$$

Using the vector relation

$$\nabla \times \nabla \times \vec{E} = \nabla(\nabla \cdot \vec{E}) - \nabla^2 \vec{E}$$

$$\nabla \times (\nabla \times \vec{E}) = \nabla \times \left(-\frac{1}{c}\frac{\partial \vec{H}}{\partial t}\right) = -\frac{1}{c^2}\frac{\partial^2 \vec{D}}{\partial t^2}$$

and noting

$$\nabla \cdot \vec{E} = \nabla \cdot \left(\frac{\vec{D}}{\varepsilon}\right) = \vec{D} \cdot \nabla\left(\frac{1}{\varepsilon}\right) + \frac{1}{\varepsilon}(\nabla \cdot \vec{D})$$

3.3 S. P. Gill, U.S. Office of Naval Research Contract Nonr 1866(24) NR-384-903, Tech. Memo. 58 (1964).

3.4 M. V. Berry The Diffraction of Light by Ultrasound, Academic Press, London (1966).

3.5 W. R. Klein and B. D. Cook, IEEE Trans. on Sonic and Ultrasonics SU-14, 123 (1967).

$$= \vec{D} \cdot \frac{1}{\varepsilon^2} \nabla\varepsilon$$

we obtain

$$\nabla^2 \vec{E} - \nabla\left(\frac{1}{c^2} \vec{D} \cdot \nabla\varepsilon\right) = \frac{1}{c^2} \frac{\partial^2 \vec{D}}{\partial t^2} \qquad (3.2\text{-}2)$$

For the geometry shown in Figure 2.1 on page 41 , we see that $\vec{D}$ is perpendicular to $\nabla(1/\varepsilon)$; therefore 3.2-2 can be reduced to

$$\nabla^2 \vec{E} = -\frac{\omega^2}{c^2} \varepsilon \vec{E} \qquad (3.2\text{-}3)$$

If $\vec{D}$ is in the plane of incidence, it can be shown, by assuming that $\vec{D}$ has a variation of $e^{i\vec{k}\cdot\vec{x}}$ in space,

$$\nabla\left(\frac{1}{\varepsilon^2} \vec{D} \cdot \nabla\varepsilon\right) = 0 \; (\Delta\varepsilon \; K/k)\nabla^2 E$$

and may therefore be neglected*.

From Chapter Two, the index of refraction of a grating is of the form:

$$n = n_1 + \eta(1+M'\cos Kx) = n_1 + (\eta' + i\eta'')(1+M'\cos Kx)$$

$$\varepsilon = \varepsilon_1 + \Delta\varepsilon(1+M'\cos Kx) = \varepsilon_1 + (\Delta\varepsilon' + i\Delta\varepsilon'')(1+M'\cos Kx) \qquad (3.2\text{-}4)$$

Substituting into equation 3.2-3, one obtains

$$\frac{\partial^2 E_z}{\partial x^2} + \frac{\partial^2 E_z}{\partial y^2} + \frac{\omega^2}{c^2} \{\varepsilon_1 + \Delta\varepsilon[1 + \frac{1}{2} M'(e^{iKx} + e^{-iKx})]\} E_z = 0 \qquad (3.2\text{-}5)$$

---

*It will be shown later in the discussion that for the worst case encountered in holographic gratings, $\Delta\varepsilon \; K/k$ is about 0.01 .

Assuming that E_z is composed of a spectrum of plane waves in the form

$$E_z = \sum_{\ell}^{\infty} i^{\ell} e^{i(\bar{k} \sin \bar{\theta} x + \bar{k} \cos \bar{\theta} y) + i\ell Kx} U_{\ell}(y)$$

$$(\ell = 0, \pm 1, \pm 2, \cdots) \qquad (3.2\text{-}6)$$

where $\bar{k} = nk = (n_1 + \eta)k$ and $n_o \sin \theta = n \sin \bar{\theta} = (n_1 + \eta) \sin \bar{\theta}$. This expansion is a logical one, since it takes into account both the oblique angle of incidence and the periodicity of the diffraction grating.

Substituting 3.2-6 into 3.2-5 and equating the coefficient of each exponential to zero, we obtain

$$\ddot{U}_{\ell}(y) + 2i\bar{k} \cos \bar{\theta}\, \dot{U}_{\ell}(y) - (2\ell \bar{k} K \sin \bar{\theta} + \ell^2 K^2)\, U_{\ell}(y) +$$

$$\frac{1}{2} i\bar{k}^2 M' \Delta\varepsilon/(\varepsilon_1 + \Delta\varepsilon)[U_{\ell+1}(y) - U_{\ell-1}(y)] = 0 \qquad (3.2\text{-}7)$$

with the boundary conditions

$$U_o(0) = 1$$

$$U_{\ell \neq 0}(0) = 0 \qquad \text{and} \qquad \dot{U}_{\ell}(0) = 0$$

The intensity in each diffracted order is given by

$$P_{\ell}(y) = U_{\ell}(y)\, U_{\ell}^{*}(y) \left| e^{i(\bar{k} \sin \bar{\theta} x + \bar{k} \cos \bar{\theta} y)} \right|^2$$

For the lossless case, the above equation is reduced to

$$P_{\ell} = U_{\ell}(y)\, U_{\ell}^{*}(y) \qquad (3.2\text{-}8a)$$

If the grating is lossy, $\bar{k}$, $\sin\bar{\theta}$, and $\cos\bar{\theta}$ all become complex and it can be shown that the exponential factor can be simplified to

$$\left| e^{i(\bar{k}\sin\bar{\theta}x + \bar{k}\cos\bar{\theta}y)} \right|^2 = e^{-2kNq(\kappa\cos\gamma + \sin\gamma)y}$$

where

$$N = (n_1 + \eta') \simeq (n_1 + \frac{1}{2}\Delta\varepsilon' / n_1)$$

$$\kappa = \eta''/n_1 \simeq \Delta\varepsilon'' / (2n_1^2 + \Delta\varepsilon')$$

$$q = \left[1 - \frac{2(1-\kappa^2)}{N^2(1+\kappa^2)^2}\sin^2\theta + \frac{(1+\kappa^2)^2}{N^4(1+\kappa^2)^4}\sin^4\theta \right]^{1/4}$$

and

$$\gamma = \frac{1}{2}\tan^{-1}\left\{ \frac{2\kappa}{N^2(1+\kappa^2)^2}\sin^2\theta \Big/ \left[1 - \frac{1-\kappa^2}{N^2(1+\kappa^2)^2}\sin^2\theta \right] \right\} \qquad (3.2\text{-}8b)$$

This is analogous to the results given on page 616 of Ref. (2.2) on propagation through metallic media*.

Various numerical techniques have been used to solve 3.2-7 and it was found that a more convenient variable to use is

$$\chi = \frac{1}{2} y\, \bar{k}\, M'\Delta\varepsilon \sec\bar{\theta} / (\varepsilon_1 + \Delta\varepsilon)$$

---

* If the gelatine is also lossy, equation 3.2-4 is modified to $n = (n_1' + in_1'') + (\eta' + i\eta'')(1+M'\cos Kx)$, $\therefore \kappa = (n_1'' + \eta'')/n_1'$ and all the n_1 in the above equation are changed to n_1'. In view of equation 2.3-7, we can also take into account of the loss due to M' smaller than unity by including the factor $\eta(1-M')$ into n_1. This enables us to include loss due to the grains into the loss due to the gelatin.

Changing the variable in equation 3.2-7, we obtain

$$\frac{1}{2} i M'\Delta\varepsilon \sec^2\bar{\theta}/(\varepsilon_1 + \Delta\varepsilon) U_\ell(\chi) - 2U_\ell(\chi) - U_{\ell+1}(\chi) + U_{\ell-1}(\chi)$$

$$-2i(\varepsilon_1 + \Delta\varepsilon)/(M'\Delta\varepsilon) \{ 2\ell K/\bar{k} \sin\bar{\theta} + \ell^2K^2/\bar{k}^2 \} U_\ell(\chi) = 0 \qquad (3.2\text{-}9)$$

In the next section, approximate solutions of 3.2-9 under various conditions will be derived and their validity discussed. It has been implicitly assumed in the derivations leading to equation 3.2-9 that the grating is immersed in a liquid with a dielectric constant $(\varepsilon_1 + \Delta\varepsilon)$ and a plane wave incident upon the grating at an angle $\bar{\theta}$ at $y = 0$. The difference in the indices of refraction for $y > 0$ and $y \leq 0$ is only the small index modulation; therefore the reflection between interfaces is neglected. The equation can then be solved assuming that the grating extends to $y = \infty$. For a grating with finite thickness L, the diffraction intensity is simply evaluated at $y = L$ and again we neglect the reflection at the interfaces of $L > y \leq L$. The actual angle of incidence θ and the diffracted angles can be compensated for by using Snell's law. If more accurate expressions for the amplitudes are desired, a correction factor taking into account the multiple reflections for each diffracted beam has to be included (3.6). For the specific case of photographic gratings, the emulsion coating usually has a glass back-plate which must also be taken into account.

3.6 H. Kogelnik, JOSA 57, 431 (1967).

This method of approach is also very convenient in obtaining the direction of propagation of the emerging plane waves at $y = L$. By substituting $y = L$ into equation 3.2-6 we see immediately that

$$\sin \theta_\ell - \sin \theta = \ell K/k$$

where θ_ℓ is the direction of propagation of the ℓth order diffracted beam.

Equation 3.2-9 will be referred to as the Raman-Nath equation, although in their original work the second derivative term was dropped out because the value of $\Delta\varepsilon$ which they were interested in was much smaller.

3.3 An Exact Formal Solution of the Raman-Nath Difference Differential Equation

The geometry involved in this diffraction problem as described in the previous section, with the grating extending from $y = 0$ to $y = \infty$, is particularly suitable to the use of the Laplace transformation to reduce it into an algebraic problem. Taking the Laplace transformation of 3.2-9 and applying the proper boundary conditions

$$Ap^2V_\ell(p) - 2pV_\ell(p) - V_{\ell+1}(p) + V_{\ell-1}(p) - B_\ell V_\ell(p) = (Ap - 2)\delta_{\ell,0} \quad (3.3\text{-}1)$$

where $V_\ell(p) = \int_0^\infty U_\ell(\chi)\, e^{-p\chi}\, d\chi$

$$A = \frac{1}{2}\, iM'\Delta\varepsilon \sec^2\bar{\theta} / (\varepsilon_1 + \Delta\varepsilon)$$

$$B_\ell = 2i(\varepsilon_1 + \Delta\varepsilon)(2\ell K/\bar{k} \sin \bar{\theta} + \ell^2K^2/\bar{k}^2)/(M'\Delta\varepsilon)$$

Equation 3.3-1 can be regrouped to form

$$C_\ell V_\ell(p) - V_{\ell+1}(p) + V_{\ell-1}(p) = (Ap - 2)\delta_{\ell,0} \qquad (3.3\text{-}2)$$

where $C_\ell = Ap^2 - 2p - B_\ell$

Equation 3.3-2 can now be solved as an algebraic equation using the standard matrix method. The use of the matrix method in connection with this problem was first published by Extermann (3.7) and was also used by Gill (3.3)

$$\begin{bmatrix}
\cdot & 0 & 0 & 0 & 0 & 0 & 0 & 0 & 0 & 0 & 0 \\
 & \cdot & 1 & 0 & 0 & 0 & 0 & 0 & 0 & 0 & 0 \\
 & -1 & C_3 & 1 & 0 & 0 & 0 & 0 & 0 & 0 & 0 \\
0 & 0 & -1 & C_2 & 1 & 0 & 0 & 0 & 0 & 0 & 0 \\
0 & 0 & 0 & -1 & C_1 & 1 & 0 & 0 & 0 & 0 & 0 \\
0 & 0 & 0 & 0 & -1 & C_0 & 1 & 0 & 0 & 0 & 0 \\
0 & 0 & 0 & 0 & 0 & -1 & C_{-1} & 1 & 0 & 0 & 0 \\
0 & 0 & 0 & 0 & 0 & 0 & -1 & C_{-2} & 1 & 0 & 0 \\
0 & 0 & 0 & 0 & 0 & 0 & 0 & -1 & C_{-3} & 1 & 0 \\
0 & 0 & 0 & 0 & 0 & 0 & 0 & 0 & -1 & \cdot & \\
0 & 0 & 0 & 0 & 0 & 0 & 0 & 0 & 0 & & \cdot
\end{bmatrix}
\begin{bmatrix} \cdot \\ \cdot \\ V_3 \\ V_2 \\ V_1 \\ V_0 \\ V_{-1} \\ V_{-2} \\ V_{-3} \\ \cdot \\ \cdot \end{bmatrix}
=
\begin{bmatrix} 0 \\ 0 \\ 0 \\ 0 \\ 0 \\ (Ap-2) \\ 0 \\ 0 \\ 0 \\ 0 \\ 0 \end{bmatrix}$$

$\Delta_3\ \Delta_2\ \Delta_1$ and $\Delta_{-1}\ \Delta_{-2}\ \Delta_{-3}$ mark the nested determinants.

(3.3-3)

Equation 3.3-3 is broken up into nested determinants to make the solutions in a more compact form. It can be solved by using the Cramer's

---

3.7 R. Extermann and G. Wannier, Helv. Phys. Acta 9, 520 (1936)

rule in a straightforward manner.

$$V_o(p) = (Ap - 2)\,\Delta_1\,\Delta_{-1} / D$$

$$V_1(p) = -(Ap - 2)\,\Delta_2\,\Delta_{-1} / D = -\Delta_2/\Delta_1\, V_o(p)$$

$$V_2(p) = (Ap - 2)\;\Delta_3\Delta_{-1} / D = -\Delta_3/\Delta_2\, V_1(p)$$

$$\vdots$$

$$V_\ell(p) = (-1)\,(Ap-2)\,\Delta_{\ell+1}\,\Delta_{-1} / D = -\Delta_{\ell+1}/\Delta_\ell V_{\ell-1}(p)$$

where $\ell = 0,1,2,\cdots$

$$V_{-1}(p) = (Ap - 2)\Delta_1\Delta_{-2} / D = \Delta_{-2}/\Delta_{-1}\, V_o(p)$$

$$V_{-2}(p) = (Ap - 2)\Delta_1\Delta_{-3} / D = \Delta_{-3} / \Delta_{-2}\, V_{-1}(p)$$

$$\vdots$$

$$V_{-\ell'}(p) = (Ap - 2)\Delta_1\Delta_{-\ell'-1} / D = \Delta_{-\ell'-1} / \Delta_{-\ell'} V_{-\ell'+1}(p) \qquad (3.3\text{-}4)$$

where $\ell' = 0,1,2,\cdots$ and $D = C_o\Delta_1\,\Delta_{-1} + \Delta_2\,\Delta_{-1} + \Delta_1\,\Delta_{-2}$ *

The inverse Laplace transformation of equations in 3.3-4 constitutes a formal solution to the Raman-Nath equation. Writing out the various terms of 3.3-4 in more detail we have

---

*We remark that 3.3-4 is not directly applicable when truncation takes place at $\ell = 1,-1$ because D contains Δ_2 and Δ_{-2}. But this is a simple situation where one does not need to express the solution in such general form.

$$\Delta_2/\Delta_1 = \cfrac{1}{C_1 + \cfrac{1}{C_2 + \cfrac{1}{C_3 + \cdot}}} \cdot$$

$$= \lim_{\ell \to N} \frac{1}{C_1^+} \frac{1}{C_2^+} \frac{1}{C_3^+} \cdots \frac{1}{C_\ell^+} \qquad (3.3\text{-}5)$$

where N is the largest ℓ retained for a truncated matrix

$$\Delta_3/\Delta_2 = \lim_{\ell \to N} \frac{1}{C_2^+} \frac{1}{C_3^+} \frac{1}{C_4^+} \cdots \frac{1}{C_\ell^+} \qquad (3.3\text{-}6)$$

$$\Delta_N/\Delta_{N-1} = \frac{1}{C_{N-1}^+} \frac{1}{C_N} \qquad (3.3\text{-}7)$$

$$\therefore \quad \Delta_1 = \left(\frac{\Delta_1}{\Delta_2}\right) \left(\frac{\Delta_2}{\Delta_3}\right) \cdots \left(\frac{\Delta_{N-1}}{\Delta_N}\right) \Delta_N$$

$$= \left(C_1 + \frac{1}{C_2^+} \frac{1}{C_3^+} \cdots \frac{1}{C_N}\right) * \left(C_2 + \frac{1}{C_3^+} \frac{1}{C_4^+} \cdots \frac{1}{C_N}\right) *$$

$$\cdots \left(C_{N-1} + \frac{1}{C_N}\right) * C_N \qquad (3.3\text{-}8)$$

$$\Delta_2 = \left(C_2 + \frac{1}{C_3^+} + \frac{1}{C_4^+} \cdots \frac{1}{C_N}\right) * \left(C_3 + \frac{1}{C_4^+} \frac{1}{C_5^+} \cdots \frac{1}{C_N}\right) *$$

$$\cdots \left(C_{N-1} + \frac{1}{C_N}\right) * C_N \qquad (3.3\text{-}9)$$

Similarly,

$$\frac{\Delta_{-2}}{\Delta_{-1}} = \frac{1}{C_{-1}^+} \frac{1}{C_{-2}^+} \frac{1}{C_{-3}^+} \cdots \frac{1}{C_{-N}}, \qquad (3.3\text{-}10)$$

$$\Delta_{-1} = (C_{-1} + \frac{1}{C^+_{-2}}\frac{1}{C^+_{-3}} \cdots \frac{1}{C_{-N'}})*(C_{-2} + \frac{1}{C^+_{-3}}\frac{1}{C^+_{-4}} \cdots \frac{1}{C_{-N'}})*$$

$$\cdots (C_{-N'+1} + \frac{1}{C_{-N'}})* C_{-N'} \qquad (3.3\text{-}11)$$

Parenthetically we remark that it is not necessary for N' to equal N.

As it stands, 3.3-4 is difficult to work with and an exact inverse transformation is difficult, if not impossible, to obtain. In the following sections we will attempt inverse transformation of 3.3-4 under special conditions.

3.4 An Approximate Solution of the Raman-Nath Equation: Phase Modulation Only

For the special case when we reduce equation 3.2-9 to

$$2\dot{U}_\ell(\chi) + U_{\ell+1}(\chi) - U_{\ell-1}(\chi) = 0 \qquad (3.4\text{-}1)$$

then

$$C_\ell = -2p$$

$$V_o(p) = -2\,\Delta_1\Delta_{-1}/D = (Ap-2)/(C_o + \Delta_2/\Delta_1 + \Delta_{-2}/\Delta_{-1})$$

$$= -2/(C_o + \frac{1}{C^+_1}\frac{1}{C^+_2}\frac{1}{C^+_3}\cdots\frac{1}{C_\infty} + \frac{1}{C^+_{-1}}\frac{1}{C^+_{-2}}\cdots\frac{1}{C_{-\infty}})$$

$$= \frac{1}{p^+}\frac{1}{2p^+}\frac{1}{2p^+}\frac{1}{2p^+}\cdots \qquad (3.4\text{-}2)$$

By using an identity for this continued fraction expression (3.8), we obtain

$$V_o(p) = 1/(p^2 + 1)^{1/2} \tag{3.4-3}$$

Similarly, substituting 3.4-3 into 3.3-4, we obtain

$$V_1(p) = -[(p^2+1)^{1/2} - p] / (p^2+1)^{1/2}$$

$$V_2(p) = [(p^2+1)^{1/2} - p]^2 / (p^2+1)^{1/2}$$

$$\vdots$$

$$V_\ell p) = (-1)^\ell [(p^2+1)^2 - p]^\ell / (p^2+1)^{1/2}$$

$$V_{-1}(p) = [(p^2+1)^{1/2} - p] / (p^2+1)^{1/2}$$

$$V_{-\ell}(p) = [(p^2+1)^{1/2} - p]^\ell / (p^2+1)^{1/2} \tag{3.4-4}$$

Taking the inverse Laplace transformation of these expressions, we obtain

$$\begin{aligned} U_o(\chi) &= J_o(\chi) \\ U_1(\chi) &= -J_1(\chi) \\ U_\ell(\chi) &= (-1)^\ell J_\ell(\chi) \\ U_{-1}(\chi) &= J_1(\chi) = -J_{-1}(\chi) \\ U_{-\ell}(\chi) &= J_\ell(\chi) = (-1)^\ell J_{-\ell}(\chi) \end{aligned} \tag{3.4-5}$$

3.8 H. S. Hall and S. R. Knight Higher Algebra, MacMillan & Company, London, 1957, p. 367.

Let us examine the validity of the solution 3.4-5. In obtaining this solution we have made certain approximations; that is, we have dropped the terms

$$A\ddot{U}_\ell(\chi) = \frac{1}{2}\, iM'\Delta\varepsilon \sec^2\bar{\theta} \,/\, (\varepsilon + \Delta\varepsilon)\, \ddot{J}_\ell(\chi)$$

and

$$B_\ell U_\ell(\chi) = 2i(\varepsilon_1 + \Delta\varepsilon)(2\ell K/\bar{k} \sin\bar{\theta} + \ell^2K^2/\bar{k}^2)/(M'\Delta\varepsilon)\, J_\ell(\chi)$$

We have substituted $J_\ell(\chi)$ into $U_\ell(\chi)$ for an order of magnitude evaluation to determine the conditions for the validity of our approximation. Using the recurrence relationship of the Bessel function, we obtain

$$B_\ell J_\ell(\chi) = 2i(\varepsilon_1 + \Delta\varepsilon)/(M'\Delta\varepsilon)$$
$$\cdot \{2K/\bar{k} \sin\bar{\theta}\ \chi[\dot{J}_\ell(\chi) + J_{\ell+1}(\chi)] + K^2/\bar{k}^2\chi[\dot{J}_\ell(\chi) + \chi\ddot{J}_\ell(\chi) + \chi J_\ell(\chi)]\} \tag{3.4-6}$$

Comparing this with $J_\ell(\chi)$ and assuming $\dot{J}_n(\chi) = O[J_n(\chi)]$, we obtain the conditions of validity for 3.4-5. They are

(i) $$\left| 8i \frac{(\varepsilon_1 + \Delta\varepsilon)\, K}{M'\Delta\varepsilon\ \ \bar{k}} \sin\bar{\theta}\ \chi \right| = 4 \tan\bar{\theta}\, L K \ll 1$$

(ii) $$\left| 2i \frac{(\varepsilon_1 + \Delta\varepsilon)\, K^2}{M'\Delta\varepsilon\ \ \bar{k}^2}\ \chi \right| = K^2 L \sec\bar{\theta}/\bar{k} \ll 1$$

(iii) $$\left| 4i \frac{(\varepsilon_1 + \Delta\varepsilon)\, K^2}{M'\Delta\varepsilon\ \ \bar{k}^2}\ \chi^2 \right| = K^2L^2M'\Delta\varepsilon \sec^2\bar{\theta}\,/(\varepsilon_1 + \Delta\varepsilon) \ll 1$$

(iv) $$A = \frac{1}{2} iM'\Delta\varepsilon \sec \bar{\theta} / (\varepsilon_1 + \Delta\varepsilon) << 1 \qquad (3.4\text{-}7)$$

These conditions are obtained directly from observations made by examining equation 3.4-6, and are not independent of each other. For example, if $\bar{\theta} > 15^\circ$ ($4 \sin 15^\circ \simeq 1$), (ii) and (iii) are automatically satisfied when (i) is satisfied. On the other hand, if $\bar{\theta} < 15^\circ$ then (i) and (iii) are automatically satisfied when (ii) is satisfied. We further note that condition (iv) is seldom violated under most experimental situations.

3.5 Approximate Solution of the Raman-Nath Equation: Bragg Region

It is observed experimentally that when a transmission grating is oriented near the Bragg angle ($K = 2k \sin \theta$), most of the diffracted power is in the 0^{th} and -1^{st} order. If we set $U_{\ell \neq 0,-1} = 0$, and in the special case where $|A| << 1$, 3.2-9 can be easily solved. The solution in this section was first derived by Phariseau (3.9) and can be deduced directly from Section 3.3 by terminating the exact solution at $N = 1$ and $N' = -2$. It can be shown that

$$V_o(p) = - \frac{2C_{-1}}{C_o C_{-1} + 1} \qquad (3.5\text{-}1)$$

and

$$V_{-1}(p) = \frac{1}{C_{-1}} V_o(p) = \frac{-2}{C_o C_{-1} + 1} \qquad (3.5\text{-}2)$$

3.9 P. Phariseau, Proc. Ind. Acad. Sc. A 44, 165 (1956).

where

$$C_o = -2p$$

$$C_{-1} = -2p - B_{-1}$$

Taking the partial fraction of the above expressions, for example the one in equation 3.5-2, we obtain

$$V_{-1}(p) = \frac{1}{2(p_1-p_2)} \left(\frac{1}{p-p_2} - \frac{1}{p-p_1}\right)$$

where

$$p_1 = \frac{1}{4} B_{-1} + \frac{1}{2} (B_{-1}^2/4 - 1)^{1/2}$$

$$p_2 = \frac{1}{4} B_{-1} - \frac{1}{2} (B_{-1}^2/4 - 1)^{1/2}$$

$$\therefore \quad U_{-1}(\chi) = \frac{1}{2(B_{-1}^2/4 - 1)} e^{1/4 B_{-1}\chi} \sin\left[\frac{1}{2} (1 - B_{-1}/4)^{1/2}\chi\right]$$

Making the substitution $B_{-1} = 4i\sigma$ we have

$$U_{-1}(\chi) = \frac{1}{2} \frac{\sin[(\sigma^2 + \frac{1}{4})^{1/2} \chi]}{(\sigma^2 + \frac{1}{4})^{1/2}} e^{i\sigma\chi} \qquad (3.5\text{-}3)$$

Similarly,

$$U_o(\chi) = \{\cos[(\sigma + \tfrac{1}{4})^{1/2} \chi] - i\sigma/(\sigma + \tfrac{1}{4})^{1/2} \sin[(\sigma + \tfrac{1}{4})^{1/2} \chi)]\} e^{i\sigma\chi} \qquad (3.5\text{-}4)$$

$U_{-2}(\chi)$ and $U_{-1}(\chi)$ may now be solved as in the method of successive approximations. Applying the result to equation 3.3-4, we obtain

$$V_{-2}(p) = \Delta_{-3}/\Delta_{-2} \, V_{-1}(p) = \frac{1}{C_{-2}} V_{-1}(p) \qquad (3.5\text{-}5)$$

$$V_1(p) = -\Delta_2/\Delta_1 \; V_o(p) = -\frac{1}{C_1} V_o(p) \tag{3.5-6}$$

where $V_o(p)$ and $V_{-1}(p)$ are assumed to be unchanged when $V_1(p)$ and $V_{-2}(p)$ appear. This is consistent with the original assumption that only $U_o(\chi)$ and $U_{-1}(\chi)$ contain any considerable amount of energy. The inverse Laplace transformation of 3.5-5 can be obtained in a straightforward manner

$$U_{-2}(\chi) = \frac{1}{4}\left[\frac{e^{ik_3\chi}}{(k_2-k_1)(k_1-k_3)} + \frac{e^{ik_2\chi}}{(k_1-k_2)(k_3-k_2)} + \frac{e^{ik_1\chi}}{(k_2-k_1)(k_3-k_1)}\right] \tag{3.5-7}$$

$$U_1(\chi) = \frac{i}{2}\left[\frac{(k_1+k_2-k_4)e^{ik_4\chi}}{(k_1-k_4)(k_2-k_4)} + \frac{k_2 e^{ik_1\chi}}{(k_2-k_1)(k_4-k_1)} + \frac{k_1 e^{ik_2\chi}}{(k_1-k_2)(k_4-k_2)}\right] \tag{3.5-8}$$

where

$$k_1 = \sigma + \sqrt{\sigma^2 + \frac{1}{4}}$$

$$k_2 = \sigma - \sqrt{\sigma^2 + \frac{1}{4}}$$

$$k_3 = 2(\rho - a \sin \bar{\theta}) = -iB_{-2}/2$$

$$k_4 = \frac{1}{2}(\rho + 2a \sin \bar{\theta})$$

$$\rho = 2(\epsilon_1 + \Delta\epsilon)/(M'\Delta\epsilon)\; K^2/\bar{k}^2$$

$$a = 2(\epsilon_1 + \Delta\epsilon)/(M'\Delta\epsilon)\; K/\bar{k}$$

$$P_o(\chi) = U_o(\chi)\, U_o^*(\chi) = \frac{1}{\sigma^2 + \frac{1}{4}} \left[\sigma^2 + \frac{1}{4} \cos^2\left[\left(\sigma^2 + \frac{1}{4}\right)^{1/2} \chi\right]\right. \tag{3.5-9}$$

$$P_{-1}(\chi) = U_{-1}(\chi)\, U_{-1}(\chi)^* = \frac{1}{4} \frac{\sin^2[(\sigma^2 + \frac{1}{4})^{1/2}\, \chi]}{(\sigma^2 + \frac{1}{4})} \tag{3.5-10}$$

$$P_{-2}(\chi) = \frac{1}{4} [(k_2-k_3)(k_1-k_3)(k_1-k_2)]^{-1}$$

$$\cdot \left\{ \frac{\sin^2[(k_3-k_2)\frac{\chi}{2}]}{k_2-k_3} + \frac{\sin^2[(k_3-k_1)\frac{\chi}{2}]}{k_3-k_1} + \frac{\sin^2[(k_1-k_2)\frac{\chi}{2}]}{k_1-k_2} \right\} \tag{3.5-11}$$

$$P_1(\chi) = \frac{1}{4} [(k_1-k_2)(k_1-k_4)(k_4-k_2)]^{-1}$$

$$\cdot \left\{ \frac{4k_1k_2\sin^2[(k_2-k_1)\frac{\chi}{2}]}{k_2-k_1} + \frac{4k_2(k_1+k_2-k_4)\sin^2[(k_1-k_4)\frac{\chi}{2}]}{k_1-k_4} \right.$$

$$\left. + \frac{4k_1(k_1+k_2-k_4)\sin^2[(k_4-k_2)\frac{\chi}{2}]}{k_4-k_2} \right\} \tag{3.5-12}$$

For the case of exact Bragg angle incidence, the expressions are considerably simpler.

$$P_o(\chi) = \cos^2(\chi/2) \tag{3.5-13}$$

$$P_{-1}(\chi) = \sin^2(\chi/2) \tag{3.5-14}$$

$$P_{-2}(\chi) = \frac{1}{4} \frac{1}{\rho^2 - \frac{1}{4}} \left\{ - \frac{\sin^2[(\rho+\frac{1}{2})\chi/2]}{\rho + \frac{1}{2}} + \frac{\sin^2[(\rho+\frac{1}{2})\chi/2]}{\rho - \frac{1}{2}} + \sin^2(\tfrac{\chi}{2}) \right\} \tag{3.5-15}$$

$$P_1(\chi) = \frac{1}{4}\frac{1}{\rho^2 - \frac{1}{4}}\left\{ - \sin^2\left(\frac{\chi}{2}\right) + \frac{2\rho}{\rho - \frac{1}{2}} \sin^2[(\rho - \tfrac{1}{2})\chi/2] \right.$$

$$\left. + \frac{2\rho}{\rho + \frac{1}{2}} \sin^2[(\rho + \tfrac{1}{2})\chi/2] \right\} \qquad (3.5\text{-}16)$$

By examining 3.5-15 and 3.5-16 we see that there are two possible conditions for P_{-2} and P_1 to be small. They are $\chi << 1$ and $\rho >> 1$. The condition $\rho >> 1$ is a more general condition than $\chi << 1$ which is of only limited interest. We shall state the conditions of validity for this solution as

$$\text{(i)} \quad |A| = |1/2\ M'\Delta\varepsilon\ \sec^2\bar{\theta}/(\varepsilon_1 + \Delta\varepsilon)| << 1$$

and

$$\text{(ii)} \quad \rho = |2(\varepsilon_1 + \Delta\varepsilon)/(M'\Delta\varepsilon)\ K^2/\bar{k}^2| >> 1 \qquad (3.5\text{-}17)$$

For the case of exact Bragg angle incidence, we can see from equation 3.5-14 that the maximum diffraction efficiency takes place at $\chi = \pi$; this implies that condition (ii) can be modified to

$$|L \sec\bar{\theta}\ K^2/(\pi\bar{k})| >> 1 \qquad (3.5\text{-}18)$$

This is comparable to the condition stated in references such as (3.5).

Equation 3.5-18 can be further simplified by the Bragg condition $K/k = 2 \sin\theta$, so that we can state it as

$$|2LK \tan\bar{\theta}/\pi| >> 1$$

$$= |8Ln_1 \sin\bar{\theta} \tan\bar{\theta}/\lambda| >> 1 \qquad (3.5\text{-}19)$$

In order to have some idea as to the value of ρ before it can be considered to be much greater than one, we plot in Figures 3.1 through 3.5 the normalized value of the diffraction efficiency; that is $P_i / \sum_{i=-2}^{1} P_i$ and the value $\sin^2(\chi/2)$ for comparison purpose. We see that for the parameters chosen here with L=60 microns, λ = 6328 Å, $n_1 = 1.5$ and $\theta = 7.5^\circ$, the solution is self-consistant in that P_{-2} and P_1 are indeed small. This corresponds to $\rho = 8.60$. For the case of $\theta = 15^\circ$ we see that the solution becomes self-consistant at L = 15 microns which corresponds to $\rho = 8.65$. From this we can conclude that the solution given by 3.5-13 and 3.5-14 are very accurate for $\rho \geq 10$.

3.6 Lossy Dielectric Gratings

In Chapter two we have studied the effective dielectric constant of a lossy medium. A more general form of the modulated index of refraction for a dielectric grating is given by equations 2.2-11 and 2.2-12. In this section we shall study the effect of loss on the diffracted power for the approximate solutions derived in the two previous sections. In most cases $\Delta\varepsilon'' = O(\Delta\varepsilon')$ so that the conditions for their validity indicated previously still apply.

Strictly speaking, in the case of a lossy grating we can no longer say phase modulation only, since there will be attenuation as the wave propagates through the grating. In this section when we say phase modulation only, we are referring to the case similar to that of Section 3.4 except the phase is now complex.

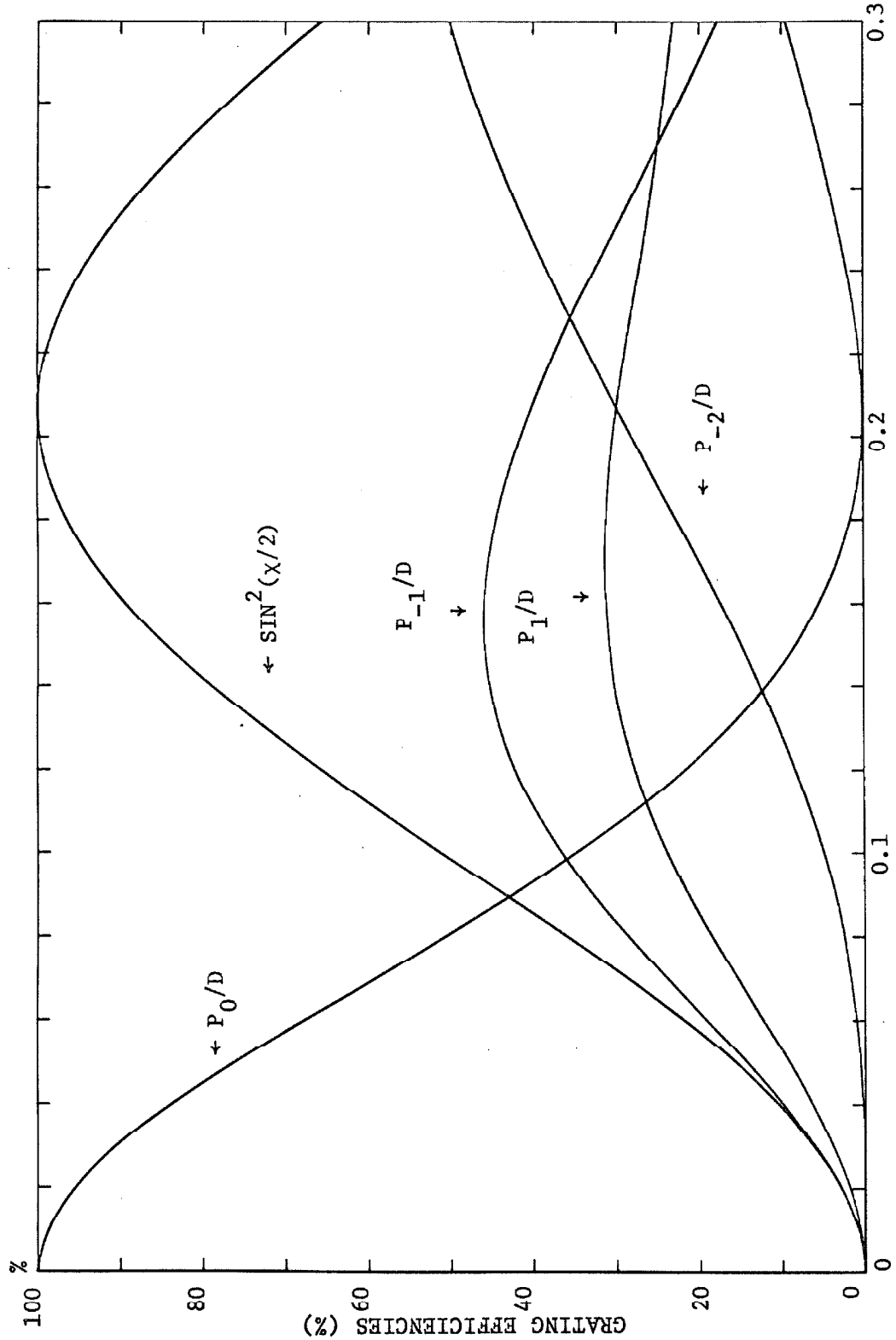

$D = P_{-2} + P_{-1} + P_0 + P_1$; $\lambda = 6328\text{Å}$; $\theta = 7.5^\circ$; $n_1 = 1.5$

FIGURE 3.1 APPROXIMATE SOLUTION; BRAGG ANGLE (Equations 3.5-12 to 3.5-16), L= 5μ.

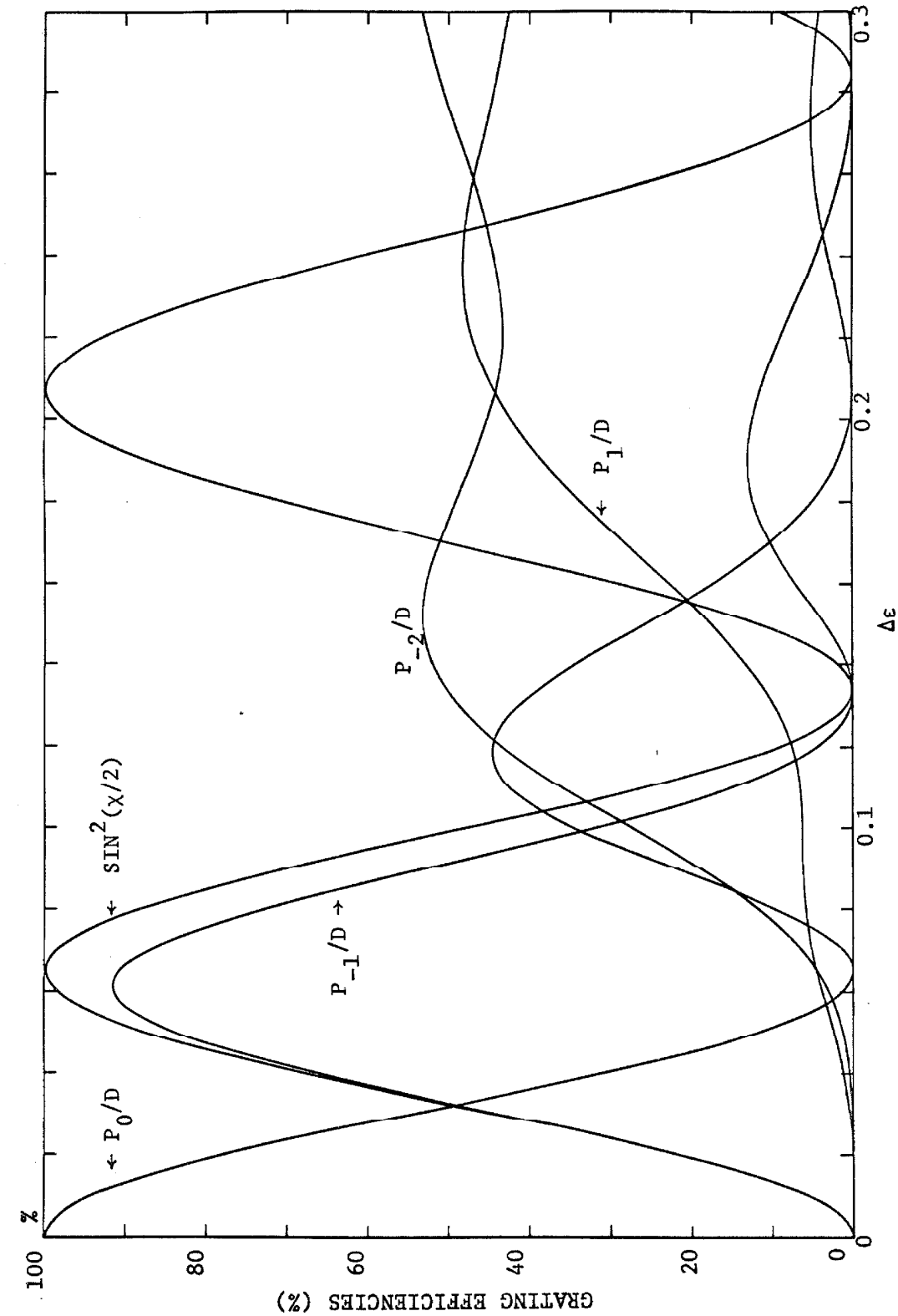

$D = P_{-2} + P_{-1} + P_0 + P_1$; $\lambda = 6328\text{Å}$; $\theta = 7.5^\circ$; $n_1 = 1.5$

FIGURE 3.2 APPROXIMATE SOLUTION: BRAGG ANGLE (Equations 3.5-12 to 3.5-16), L = 15μ

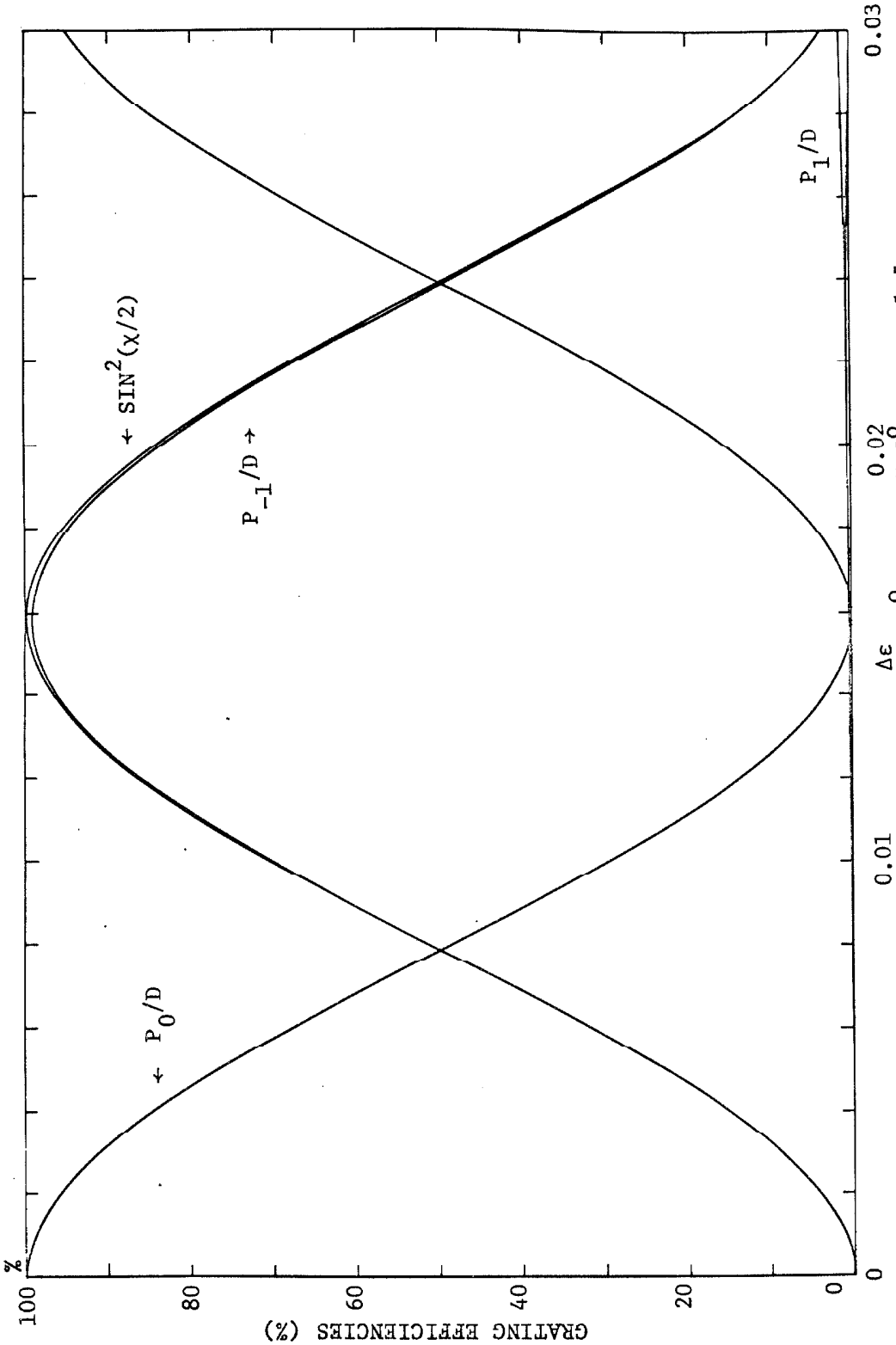

FIGURE 3.3 APPROXIMATE SOLUTION: BRAGG ANGLE (Equations 3.5-12 to 3.5-16), L =60 μ

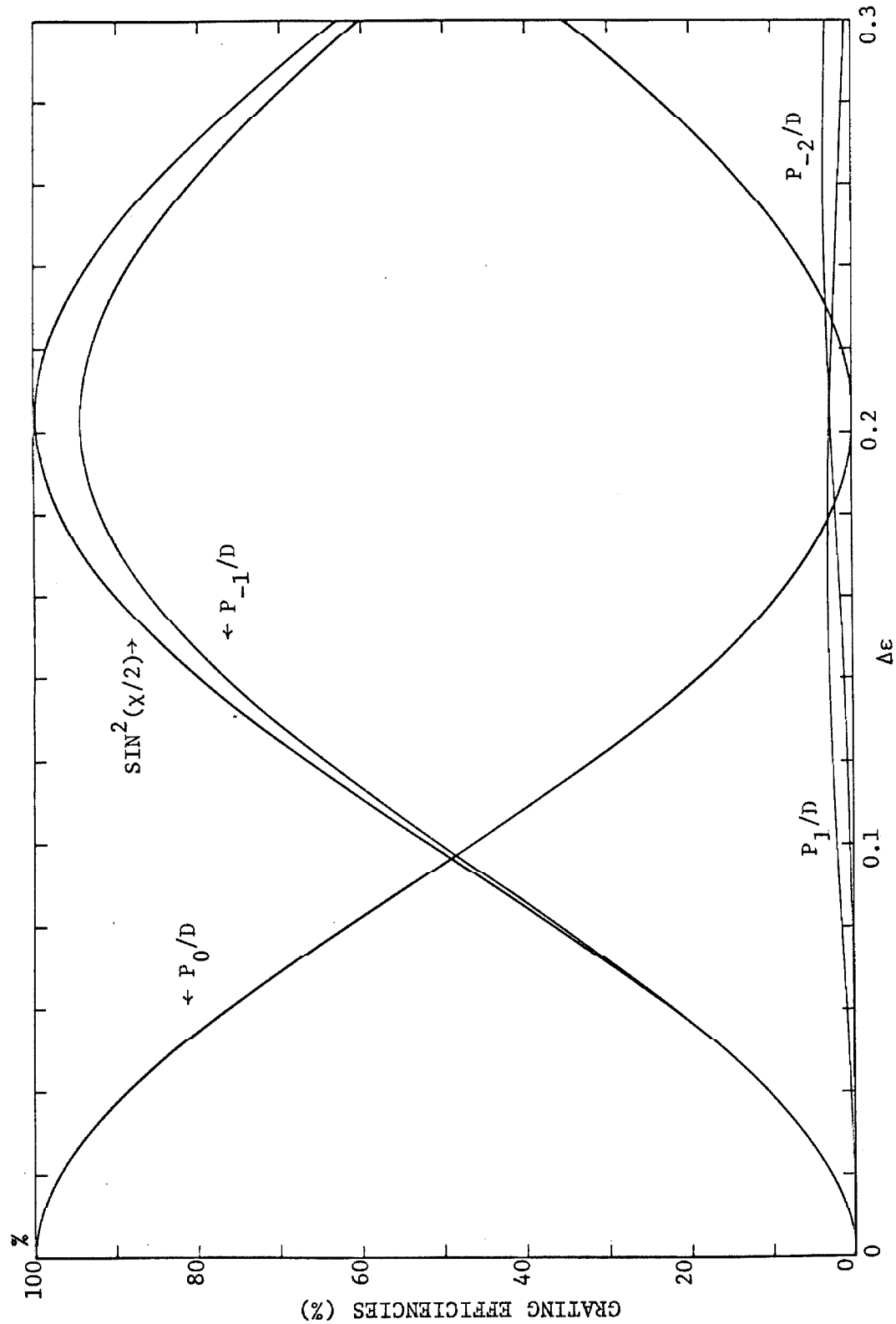

$D = P_{-2} + P_{-1} + P_0 + P_1$; $\lambda = 6328$ Å ; $\theta = 15^\circ$; $n_1 = 1.5$

FIGURE 3.4 APPROXIMATE SOLUTION: BRAGG ANGLE (Equations 3.5-12 to 3.5-16), L = 5 μ

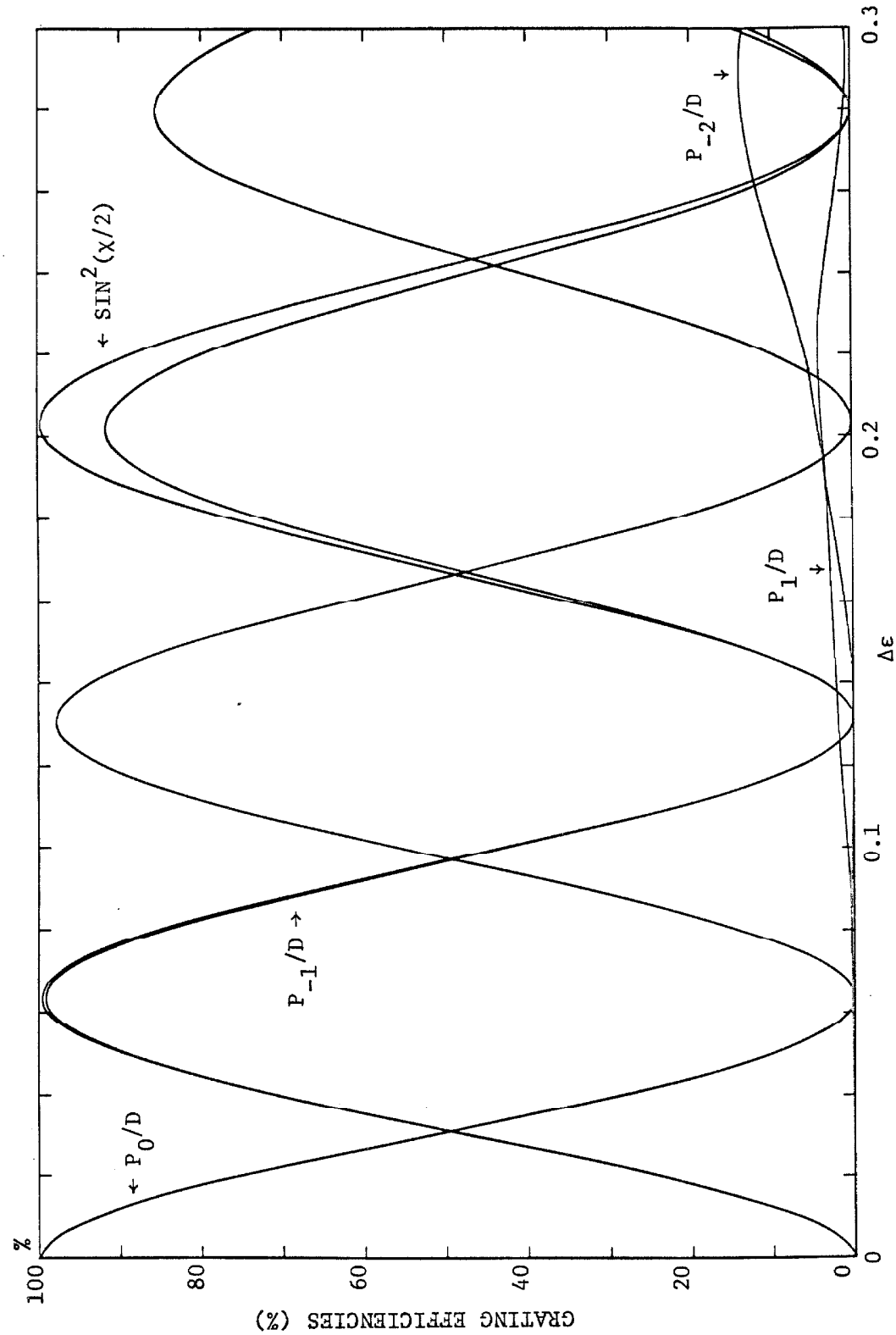

$D = P_{-2} + P_{-1} + P_0 + P_1$; $\lambda = 6328\text{Å}$; $\theta = 15^\circ$; $n_1 = 1.5$

FIGURE 3.5 APPROXIMATE SOLUTION: BRAGG ANGLE (Equations 3.5-12 to 3.5-16), L = 15 μ

Combining 3.2-8b with the solutions given in 3.4-5, we obtain the diffracted power

$$P_\ell(\chi) = |J_\ell(\chi)|^2 \, e^{-2kNq(\kappa \cos \gamma + \sin \gamma)L} \qquad (3.6\text{-}1)$$

N, q, κ and γ are defined in Section 3.2. χ is a complex number and may be written as $\chi = \chi' + i\chi''$. A useful identity for numerical computation is* (3.10)

$$J_n(\chi)\, J_n^*(\chi) = \frac{1}{\pi} \int_0^\pi J_o\{[2(\chi'^2 - \chi''^2) - 2(\chi'^2 + \chi''^2)\cos\theta]^{1/2}\}\cos n\theta \, d\theta \qquad (3.6\text{-}2)$$

A similar expression can be derived for the case where the incident angle is near the Bragg angle. At exactly the Bragg angle

$$P_{-1}(\chi) = e^{-2kNq(\kappa \cos \gamma + \sin \gamma)L} \, |\sin(\chi/2)|^2$$

$$= e^{-2kNq(\kappa \cos \gamma + \sin \gamma)L} \, [\sin^2(\chi'/2) + \sinh^2(\chi''/2)] \qquad (3.6\text{-}3)$$

Equation 3.6-3 is plotted in Figure 3.6 and we see that the exponential factor decreases more rapidly than $\sinh^2(\chi''/2)$, so that P_{-1} remains finite as the argument becomes large. Several interesting observations can be made from this graph. The peak efficiency for gratings of different thickness is the same and does not change by

---

*In most instances the computer does not handle complex numbers and has no subroutine for evaluating higher order Bessel functions.

3.10 N. N. Lebedev, Special Functions and Their Applications, Prentice-Hall (1965).

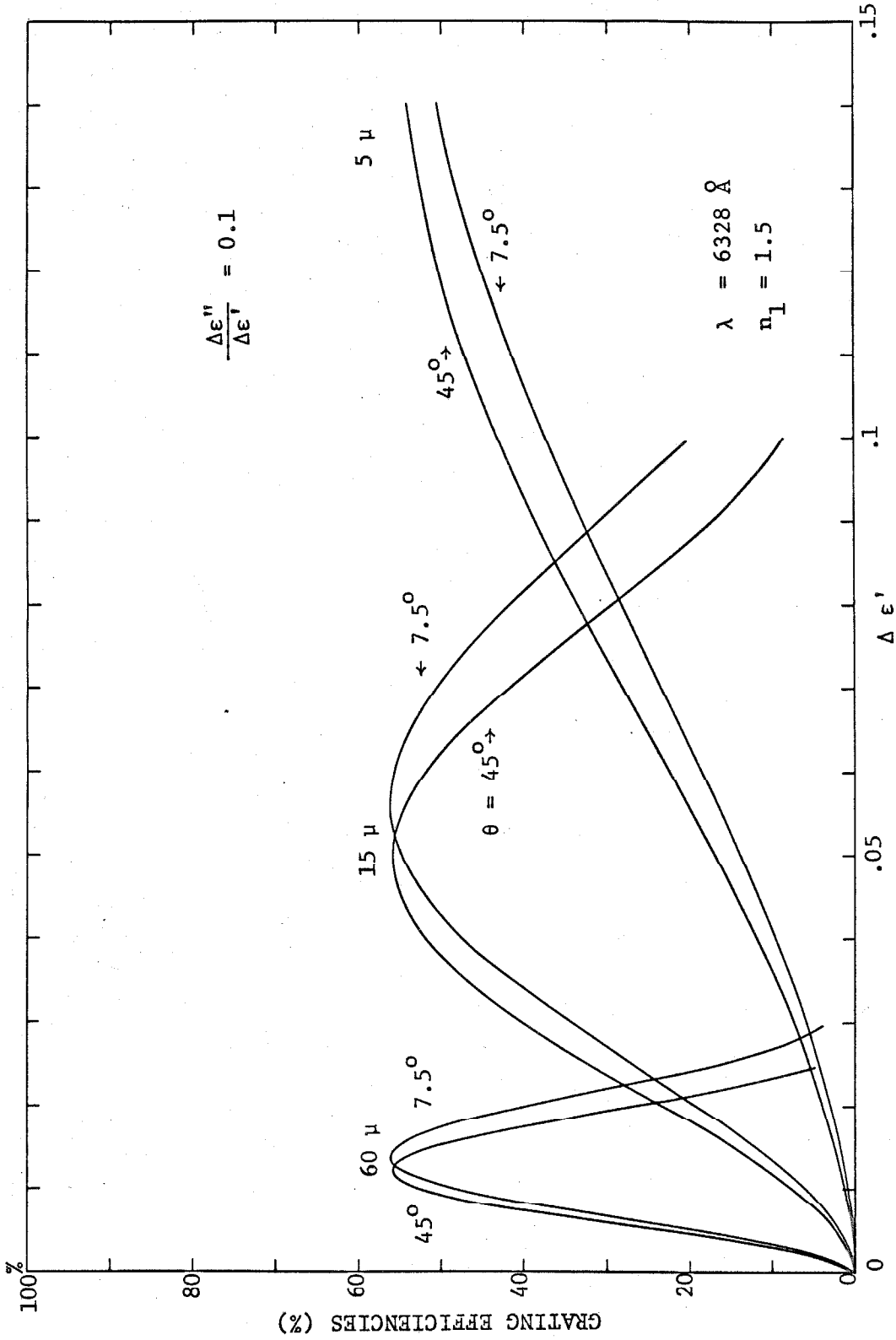

FIGURE 3.6 APPROXIMATE SOLUTION: BRAGG ANGLE (Equation 3.6-3)

increasing the spatial frequency of the grating. Increasing the thickness and the spatial frequency only changes the value of $\Delta\varepsilon$ where the peak efficiency occurs. This indicates that less exposure is needed to obtain the same optimum efficiency.

Let us examine the effect of M', the modulation transfer function, on the efficiency of a lossy grating. We see that in order to reach $\chi' = \pi$ for maximum diffraction efficiency, we have to raise $\Delta\varepsilon$ by a factor $1/M'$. The exponential factor would be a much smaller number when χ reaches π, because M' is not present in the exponential factor, which implies a decrease in the ultimate efficiency. This points to the significance of increasing the modulation transfer function, and is in agreement with the discussion given in Page 53.

3.7 Numerical Solution

In Section 3.3 we have derived an exact formal solution for the Raman-Nath equation, but it is found to be of little practical use. In Section 3.5 the method of terminating the set of infinite numbers of the difference differential equations has first been used. Its use is justified because the diffracted waves of higher orders have sufficiently small amplitudes so that they may be neglected. When more than three terms are retained, the algebra becomes extremely tedious even with this approach and it is difficult to obtain solutions in their closed form. In this section we shall discuss and describe the solutions obtained by using a digital computer. It is advantageous to use a computer because equation 3.2-7 may be solved without any simplification and it is possible to terminate the equation at any order, making the analysis applicable to all angles of incidence. The only practical

limitations are perhaps the availability of computer time and the complexity of the program.

The basic approach involves the use of the definition of derivative to evaluate the value of the function at an incremental distance away from an originating point. This value is then used to evaluate still another point. The actual technique applied in the DEQ subroutine is more sophisticated and uses the Runge-Kutta-Gill method. The DEQ subroutine also offers the option of using a variable mode, whereby the iteration interval is automatically changed when the slope between two points exceeds a predetermined value. Figures 3.7, 3.8 and 3.9 are typical computer results. In these plots the thickness y is used as the variable with $\Delta\varepsilon$ as a parameter. Only U_1, U_0, U_{-1} and U_{-2} are retained and θ is chosen to be exactly the Bragg angle.

From Figures 3.7 and 3.8 we see that for small $\Delta\varepsilon$ the curves agree favorably with the results obtained in Section 3.5 where $P_{-1} = \sin^2 \chi/2$; but as $\Delta\varepsilon$ increases as in Figure 3.9, the diffraction efficiencies depart significantly from those results. This is in agreement with the condition of validity $\rho >> 1$ which we have derived for such solutions.

The number of differential equations that should be retained still remains to be determined. We shall again resort to self-consistency as the basic requirement. That is, if we can show by an estimation that the amplitudes of the terms we have neglected are small,

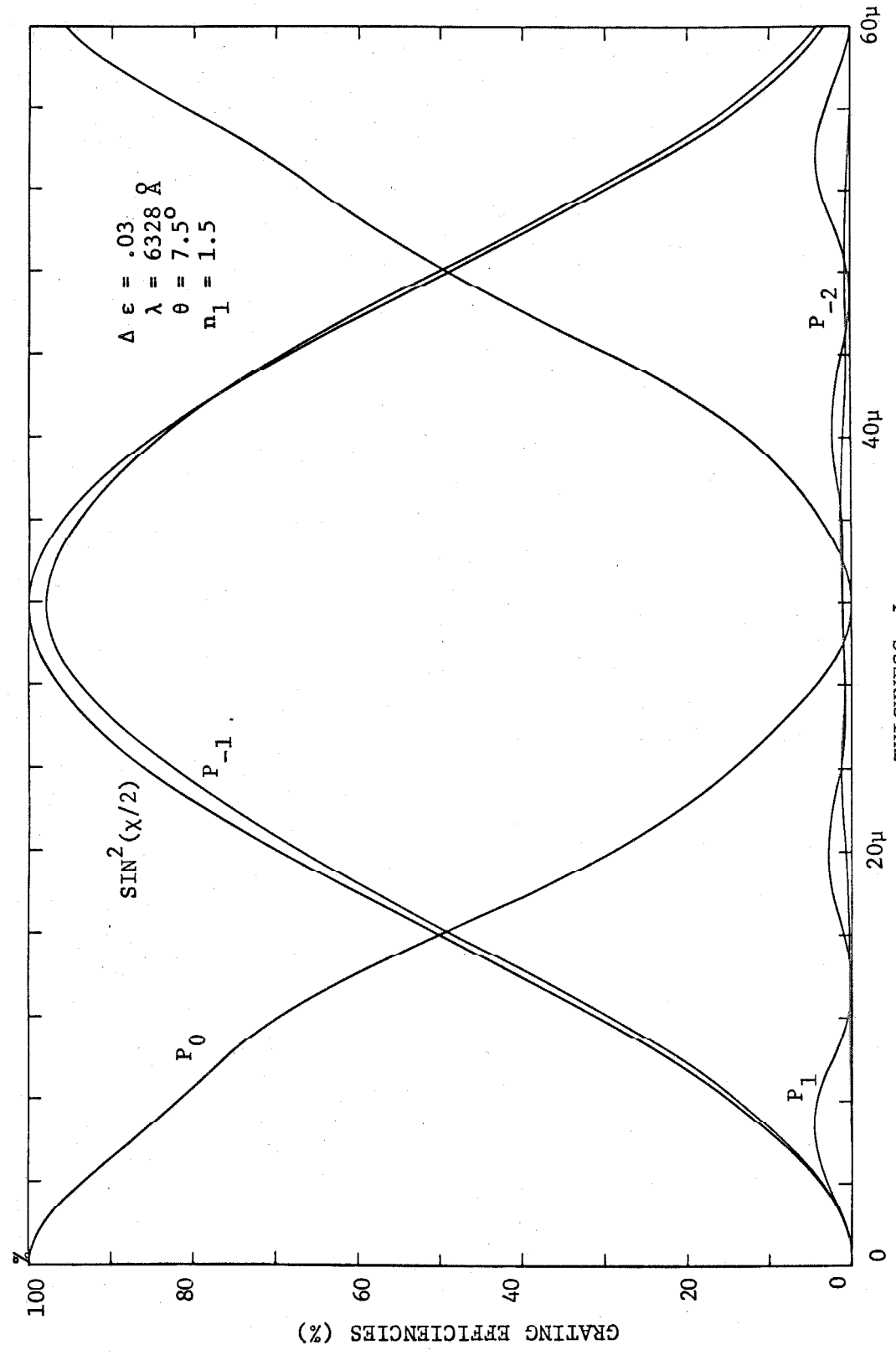

FIGURE 3.7 COMPUTER SOLUTION: FOUR COUPLED WAVE EQUATIONS $\Delta \varepsilon = .03$

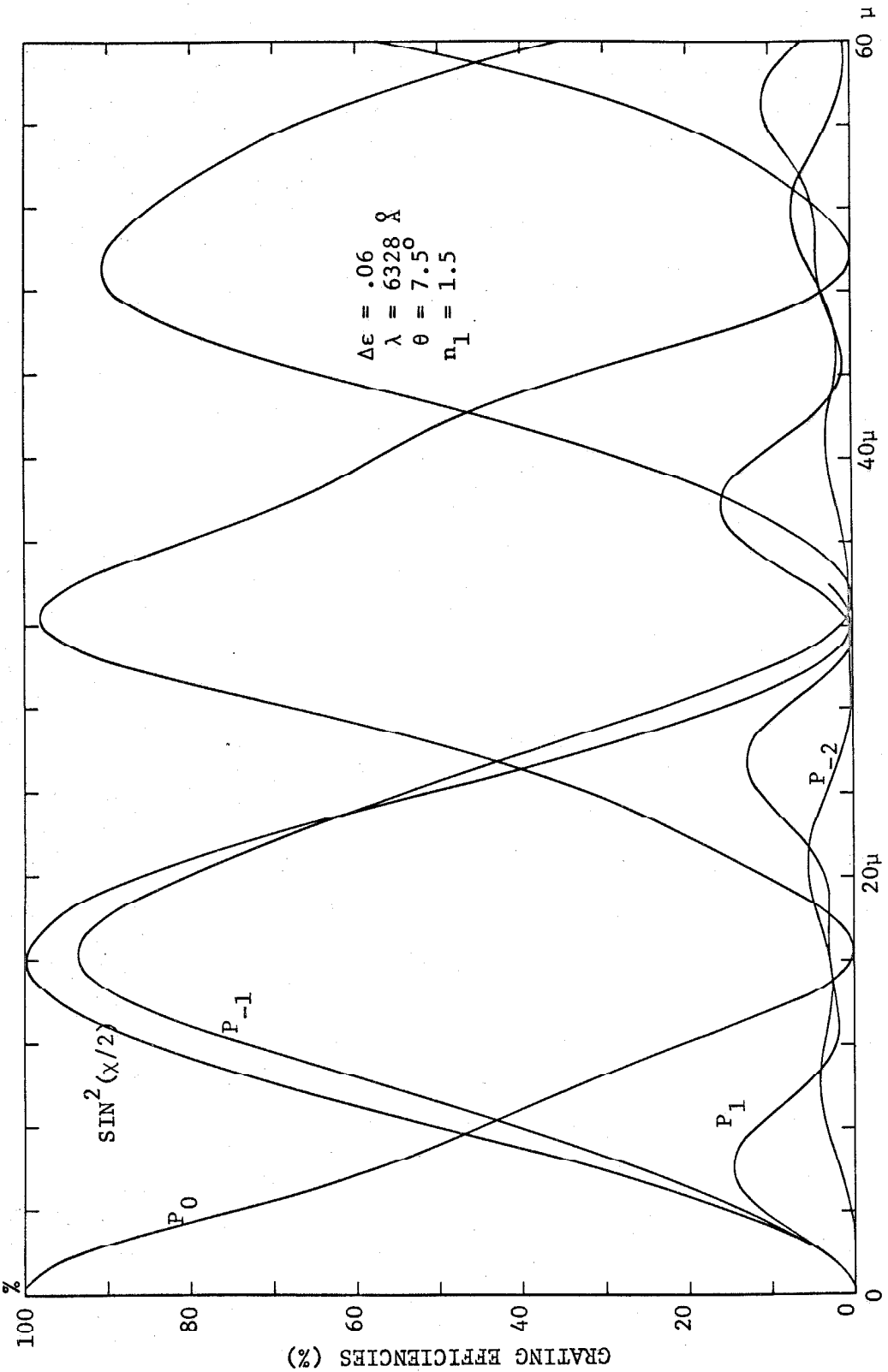

FIGURE 3.8 COMPUTER SOLUTION: FOUR COUPLED WAVE EQUATIONS $\Delta\varepsilon$=.06

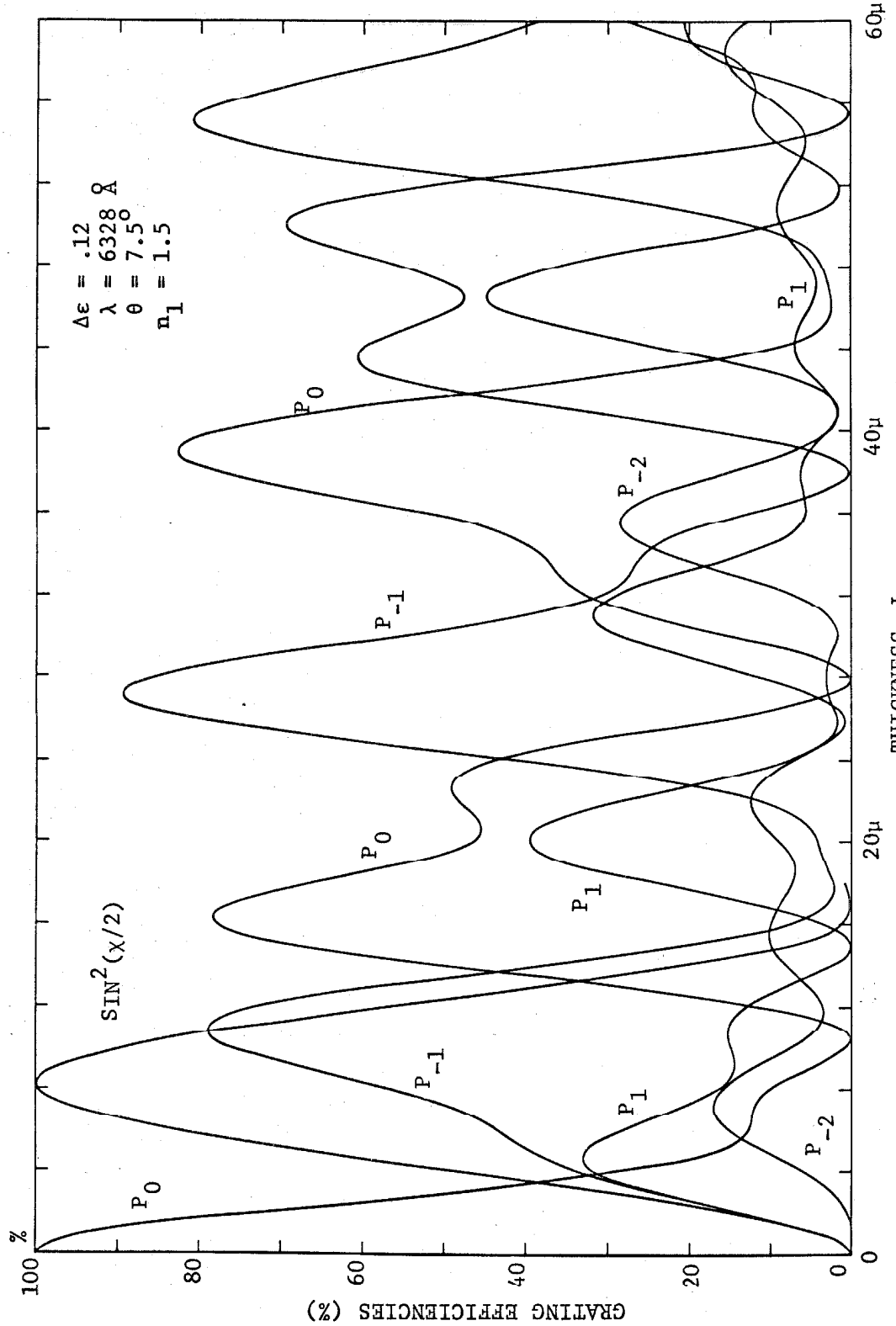

FIGURE 3.9 COMPUTER SOLUTION: FOUR COUPLED WAVE EQUATIONS $\Delta\varepsilon$ =0.12

then the truncation is justified.

Let us examine the specific case we have treated here with truncation taking place at $N=1$, $N'=-2$. From equation 3.3-4 we see that

$$V_{-3}(p) = \Delta_{-4}/\Delta_{-3}\, V_{-2}(p) = \frac{1}{C_{-3}} V_{-2}(p)$$

$$= V_{-2}(p) / (Ap^2 - 2p - B_{-3})$$

Let us specifically examine the case $\Delta\varepsilon = 0.12$. From Figure 3.9 we see that

$$V_{-2}(p) = \sum_i a_i \sin \omega_i y$$

is a reasonable expansion, and that the only a_i of any significant magnitude corresponds to $\omega_I \simeq 3$. Also for simplicity, set $A = 0$ for this error estimation.

$$V_{-3}(p) = \frac{-1}{(2p + B_{-3})} \cdot \frac{\omega_I a_I}{p^2 + \omega_I^2}$$

$$= -\left[\frac{4\omega_I a_I}{(B_{-3}^2 + 4\omega_I^2)(2p+B_{-3})} - \frac{2\omega_I a_I\, p}{(B_{-3}^2 + 4\omega_I^2)(p^2 + \omega_I^2)}\right.$$

$$\left. + \frac{B_{-3}\omega_I a_I}{(B_{-3}^2 + 4\omega_I^2)(p^2 + \omega_I^2)}\right]$$

Therefore

$$U_{-3}(\chi) \simeq -\left[\frac{2\omega_I a_I}{(B_{-3}^2 + 4\omega_I^2)} e^{-B_\ell \chi/2} - \frac{2\omega_I a_I}{(B_{-3}^2 + 4\omega_I^2)} \cos(\omega_I \chi) \right.$$

$$\left. + \frac{B_{-3} a_I}{(B_{-3}^2 + 4\omega_I^2)} \sin(\omega_I \chi) \right]$$

Noting that $B_{-3}^2 = - |B_{-3}|^2$

$$|U_{-3}| \leq |a_I| \left[\frac{4\omega_I}{4\omega_I^2 - B_{-3}^2} + \frac{|B_{-3}|}{4\omega_I^2 - B_{-3}^2} \right]$$

with the parameters chosen for this plot; $B_{-3} \simeq 10$, $\omega_I \simeq 3$

$$|U_{-3}| \leq |a_I| * [12/64 + 10/64] = |a_I| \ 22/64$$

$$|U_{-3}|^2 \leq .03$$

a_I is taken approximately as the maximum value of $|U_{-2}|$ in the region of interest. Similar derivation can be carried out for the estimation of $|U_2|$, and it is found that $|U_2|^2 = 0.02$. The higher order terms can also be estimated this way if we note that the dominant frequencies for $|U_{-3}|$ are ω_I and $B_{-3}/2$. A somewhat more general approach to amplitude estimation for higher order terms is given in Reference (3.4). It suffices to state here that they are very small, such that for the worst case, with the maximum $\Delta\varepsilon$ encountered, the total error incurred by retaining only four terms is well within 5% for the range

of thicknesses of interest.

3.8 Comparison of Results

We remark that Figures 3.8 and 3.9 depart considerably from the curves shown in Figures 3.1 to 3.5, which essentially have the simple sine-cosine variations. This is to be expected, since more "roots" are involved as the expressions in equation 3.3-4 become more complex. Figures 3.8 and 3.9 show a close resemblance to the curves obtained by Hance (3.11), who started from the simple "phase only" solution and used an iterative method to obtain his result.

The computer solution differs from the simple sinusoidal solution in several ways. As expected, the sinusoidal solution overestimates P_0 and P_{-1}. This estimation becomes worse as the value of $\Delta\varepsilon$ gets larger because the conditions restricting the validity of the sinusoidal solution are being violated. Furthermore, from these plots the values of y for the maximum efficiency, with $\Delta\varepsilon$ as a fixed parameter, are larger than those predicted by the solutions of Section 3.5. This is to be expected, because if we plot curves of efficiency versus $\Delta\varepsilon$ with y as a fixed parameter, the peaks of these curves occur at values of $\Delta\varepsilon$ smaller than those predicted by the solutions of Section 3.5. This is indeed the case, because as the thickness gets smaller, our solution approaches the Bessel function solution as predicted by Section 3.4. The first order Bessel function has a peak

---

3.11 H. V. Hance, "Light Diffraction by Ultrasonic Waves as a Multiple Scattering Process", Physics Tech. Report 6-74-64-35, Lockheed Aircraft Corp., Sunnyvale, California (1964).

at $\chi \simeq 1.85$, whereas the sine solution has its peak at $\chi = \pi$.

Figure 3.10 shows such a plot where we have used y as a fixed parameter and $\Delta\varepsilon$ as a variable. The curves are obtained by taking points from a series of computer plots similar to those of Figures 3.7, 3.8 and 3.9. From Figure 3.10 we can see that for $y = 60$ microns a peak efficiency of 98.5% can be obtained, whereas for a substrate of $y = 5$ microns, the highest obtainable efficiency is only 39.5%, which is close to the peak efficiency of 33.9% predicted from the "phase only" solution.

Similar plots have been obtained for the lossy cases, two of which are shown in Figures 3.11 and 3.12. From a series of these curves we can determine the peak efficiency for a fixed thickness and loss factor, and the result is shown in Figure 3.13.* In each of these cases the 60 micron curve fits equation 3.6-3 very well when confirming our earlier assumption that within our range of losses the conditions of validity determined for the lossless case still apply.

The same procedure can be repeated using θ as the varying parameter. In this manner we can obtain plots showing the angular dependence of the diffraction efficiency. This dependence has been treated by George (3.12) using a different approach, and has been verified experimentally.

---

*The asymptotic value of this curve should have been 6.25% for the 5 micron case. The curve shows 5%. The discrepancy is due to the simplification made in the $1/(\varepsilon_1 + \Delta\varepsilon) \simeq 1/(\varepsilon_1 + \Delta\varepsilon')$ in the expression for χ , as we did not intend to include cases involving such high loss factors at the earlier part of this study.

3.12 N. George and J. W. Matthews, Appl. Phys. Letters 9, 212 (1966).

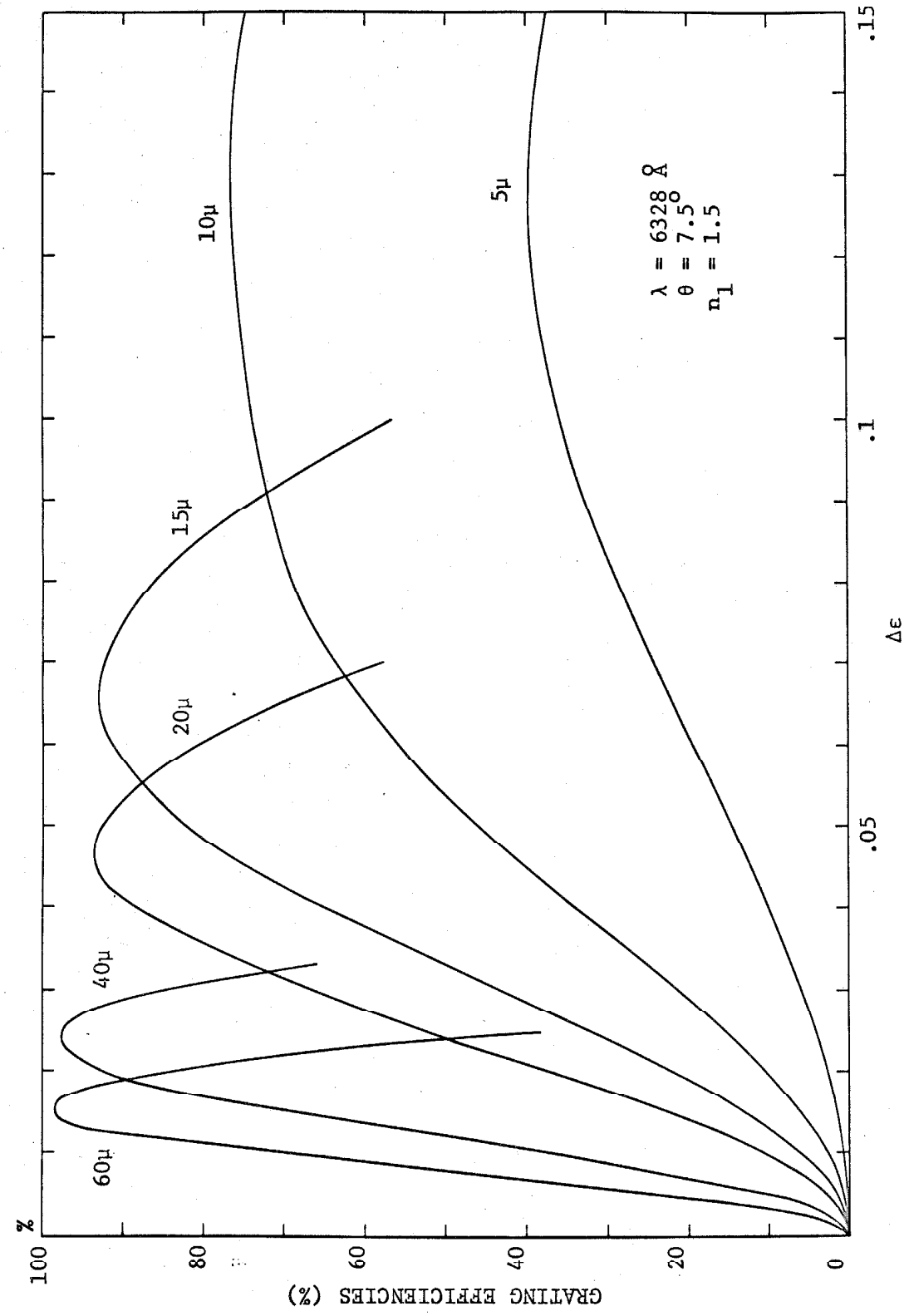

FIGURE 3.10 COMPUTER SOLUTION: FOUR COUPLED WAVE EQUATIONS, PARAMETER L

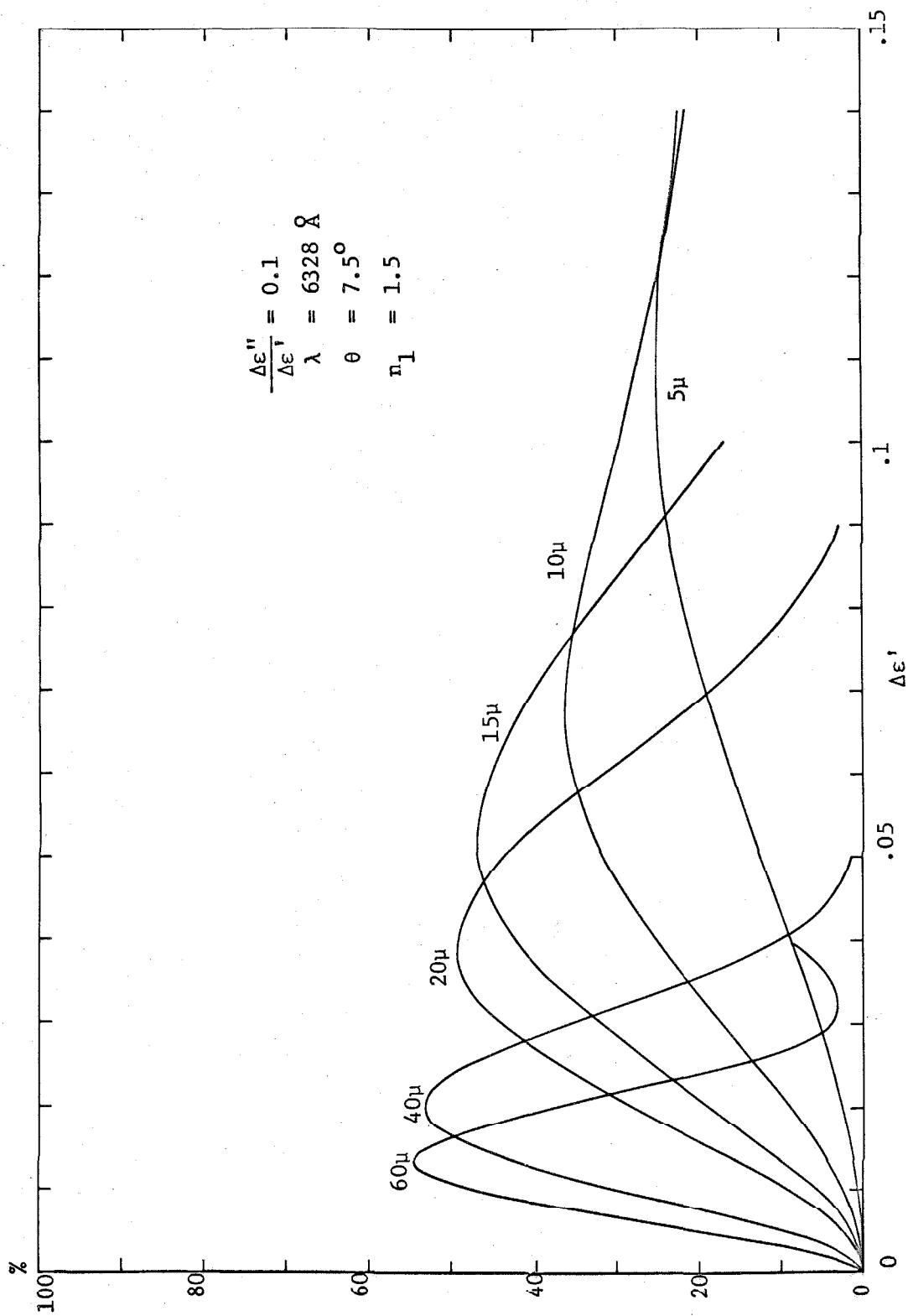

FIGURE 3.11 COMPUTER SOLUTION: FOUR COUPLED WAVE EQUATIONS, PARAMETER L

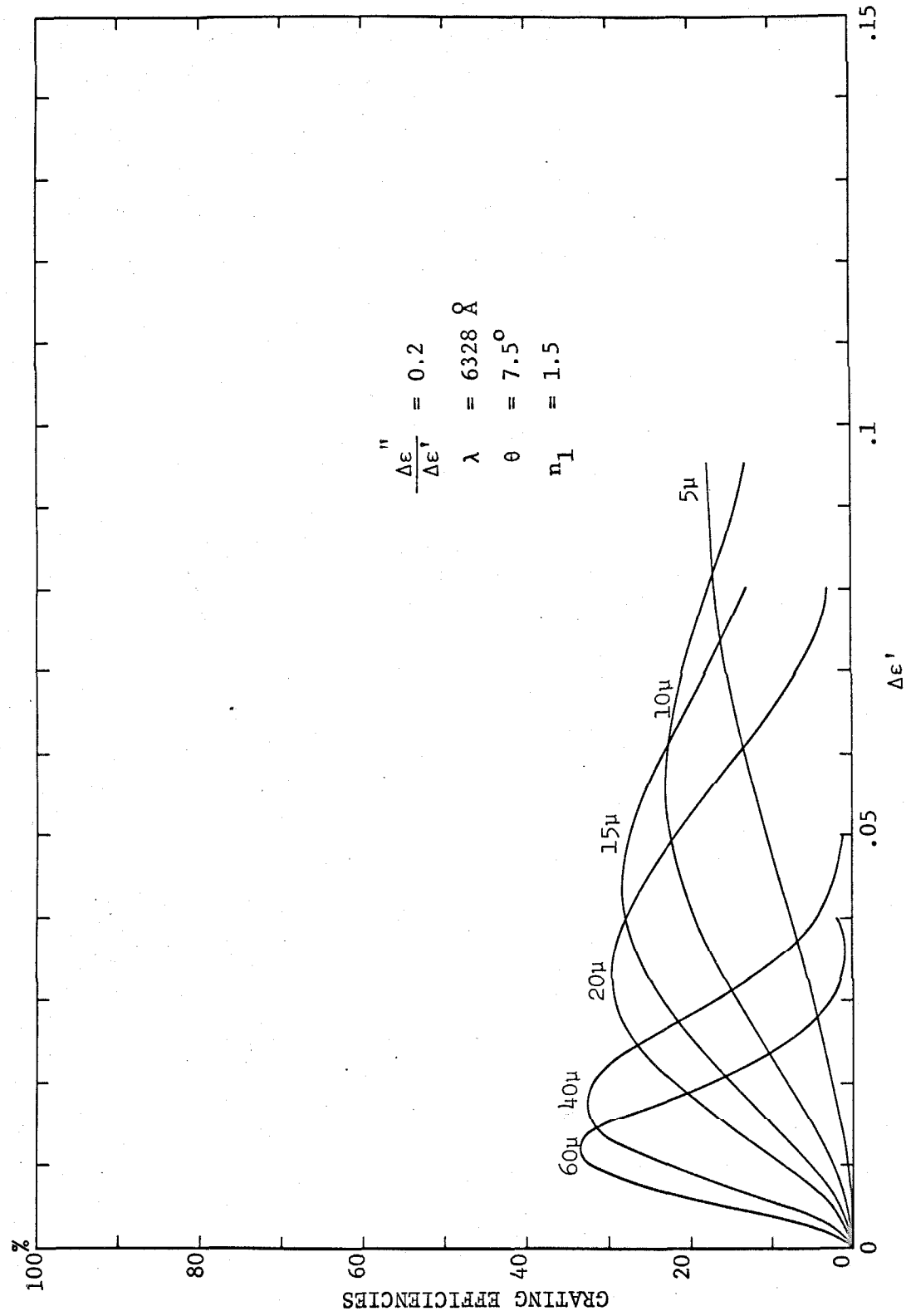

FIGURE 3.12 COMPUTER SOLUTION: FOUR COUPLED WAVE EQUATIONS, PARAMETER L

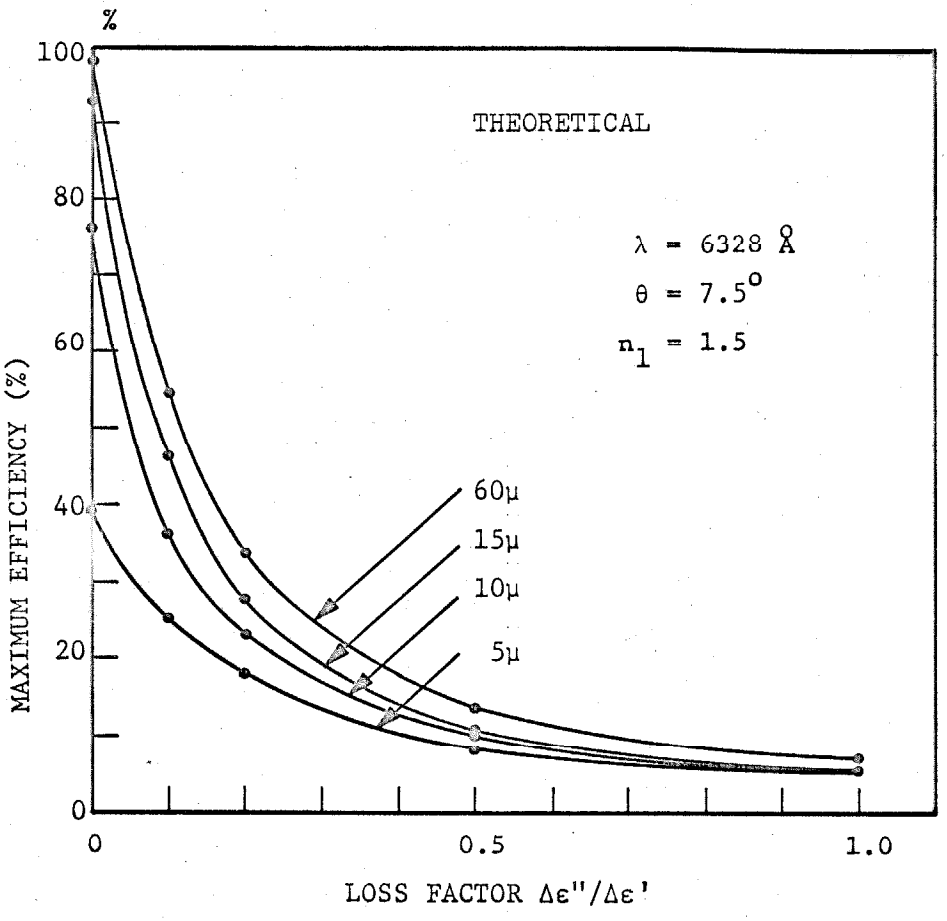

FIGURE 3.13 MAXIMUM EFFICIENCY VERSUS LOSS FACTOR FOR FIXED THICKNESS L.

Figure 3.13 is very useful in practice. If we are given an emulsion of certain thickness to evaluate its merits, we can experimentally determine the optimum efficiency by varying the exposure (see Figure 4.2). We can then estimate the loss factor $\Delta\varepsilon''/\Delta\varepsilon'$ and the optimum efficiency for any other thickness (assuming a linear density-exposure curve). If we obtain an efficiency of 26% for an emulsion of 5 microns with the parameters shown in Figure 3.13, the loss factor is about 0.1 , we can then interpolate the efficiency to be about 55% for an emulsion of 60 microns.

The usefulness of 3.13 is not limited to the parameters stated. It gives a good estimation even for other parameters so long as we keep the factor $K^2L/(k \text{ Sec } \theta)$ constant. This results from an estimation in the order of magnitude of the errors made in truncation of the coupled equations. For example, if we decrease K and increase θ in accordance with the Bragg condition, we have effectively increased the thickness, so that the above factor remains constant. For a lossy grating, M' must be included to get an accurate prediction when different spatial frequencies are involved.

CHAPTER FOUR

HIGH QUALITY GRATINGS

4.1 Introduction

We have treated three topics in the previous chapters without much correlation between them. With the knowledge gained from these topics, we are now in a position to formulate the requirements that will enable us to produce better gratings and holograms. In the first chapter we have described different holographic materials with special emphasis on photographic emulsions. Different processing techniques have been described and evaluated with reference to visual observations. In the second chapter we have determined the required characteristic curve that would enable us to produce gratings with sinusoidally modulated index of refraction. The modulation transfer function of a bleached emulsion was described and a method of improving the modulation transfer function at a specific spatial frequency has been proposed. In the third chapter, a theoretical description of the diffraction phenomena has been presented and we have determined the optimum efficiency obtainable for a fixed thickness with the assumption that the index of refraction is sinusoidally modulated. In this chapter, we will start with a discussion on the various techniques of producing high quality gratings, and state the specifications for new chemicals and new emulsions with the knowledge gained from the earlier chapters. We will then describe various experiments that we have

conducted to produce such gratings, and compared qualitatively with the theoretical calculations. We conclude this chapter and this manuscript by proposing several experiments to extend this work.

4.2 Discussion and Summary

In describing the processing technique of photographic emulsions, emphasis is placed upon how to produce dielectric gratings. From the results of Chapter Three we see that only dielectric gratings with low loss are capable of diffracting a large percentage of the incident power into the first order. However, efficiency is often not the most important criterion; equally important is the resolution of the grating. It often requires a trade off between these two factors.

In the past, when resolution was more important, the holograms were simply fixed and the bleaching process was omitted. During the latter process the grains tend to cross-link which causes severe problems, especially when a large amount of grains is present. We have solved this problem by omitting the bleaching step, using a method similar to the reversal process. We used a developed but unfixed plate and dissolved the silver grains, leaving the desirable silver halide crystals. Gratings produced in such a manner should have a better resolution than the unbleached plates, because the undeveloped grains are round, unlike the elongated "sea-weed" shaped structure of the developed silver grain. We have produced such gratings with good resolution and an efficiency of 35% on 649F plates simply by dissolving the silver with concentrated nitric acid. The presence of such volatile acids in an optical laboratory is generally undesirable as

they are dangerous to use. This really points out the need for finding a better reversal bath for the purpose described here.

By examining the micrographs of gratings produced by different processes, one can easily determine the resolution of each grating visually without actually doing an experiment to resolve two closely spaced spectral lines. If resolution is the only requirement, then certain bleaches can be immediately rejected. Similarly, if we are mainly interested in efficiency, we can make plates with the same uniform density and measure the transmittance after bleaching. This will enable us to estimate the maximum efficiency from the curves shown in Chapter Three.

We have pointed out the need to study the use of desensitizers or some other means to stabilize the grains inside the emulsion, and have demonstrated that desensitizing the gratings with the use of a dye is possible.

In Chapter Two we have correlated the index of refraction of a bleached plate to its density before bleaching, thus establishing the requirement for the characteristic curve of an emulsion that will enable us to produce gratings with a sinusoidally modulated index of refraction. The requirement is that the emulsion should have a linear density-exposure curve. The need for such a grating has been indicated in Chapter Three, where we have shown that such grating is capable of obtaining 100% efficiency for sufficiently thick substrate. Any non-linearity will only cause direct coupling between the zeroth order and the second order, reducing maximum power diffracted into the first

order. To be able to compare experimental results with our theoretical curves, one must produce gratings with a sinusoidally modulated index of refraction.

We have also obtained a relation between the modulation transfer function of a bleached and an unbleached plate. This is an important result, because there is no direct method of measuring the MTF of a bleached plate, except by tedious measurements under an interference microscope. The MTF of an unbleached plate is easily obtainable. A significant contribution presented in this connection is a method of improving the MTF at a specific spatial frequency to unity. This is indeed an exciting finding which will enable us to produce highly efficient gratings of good quality at line spacings that could not be produced by conventional methods. Furthermore, it is also applicable to holograms, if the scene subtends a small angle from the holographic plate, because the fringes recorded have a small distribution in spatial frequency with respect to the central frequency.

In the third chapter the theoretical aspects of the gratings described above are studied. Numerical solution with parameters pertinent to photographic emulsion is presented. Loss has been included in our solution since most of the bleaches produce gratings with small loss. Through this careful analysis, we are able to establish the maximum efficiency for a fixed thickness with a given loss factor. This result is summarized in Figure 3.13.

We have shown that for a lossless grating thicker than 20 microns, the efficiency is approximated by $\sin^2(\chi/2)$ where

$\chi = \frac{1}{2} y\bar{k}M'\Delta\varepsilon \text{ Sec } \bar{\theta}/(\varepsilon_1 + \Delta\varepsilon)$. For pictorial holograms the scene usually subtends over a range of θ. Both M' and Sec $\bar{\theta}$ depends on θ. In order to obtain a uniformly bright field of view, it is necessary to keep the variable χ constant over the range of $\bar{\theta}$ the object subtends. Perhaps some effort should be devoted in producing M' of a desired shape.

4.3 High Quality Gratings - Experimental Result

Gratings have been produced on 649F plates for the evaluation of various bleaches. The gratings are produced with a 6328 Å He-Ne laser, with both beams oriented at 7.5° as shown in Figure 2.1 so that the recorded spatial frequency is about 400 lines/mm. Maximum efficiencies measured with 6328 Å at Bragg angle are, 54% for chromium intensifier (Section 1.2.6.1), 40% for potassium ferricyanide-bromide bleach (Section 1.2.6.4), 23.5% for potassium ferricyanide-iodide bleach (Section 1.2.6.4) and 35% for the nitric reversal bath (Section 1.2.7.3). The gratings with the least scattering noise are those produced with the nitric acid reversal bath and the potassium ferricyanide-bromide bleach .

In order to compare experiment with theory, we have produced a series of small gratings on a 649F microflat plate which has been preflashed, and bleached with chromium intensifier for high efficiency. The measured efficiency is then plotted versus the logarithm of the exposure. As indicated in Chapter Two, we should have plotted the efficiency versus exposure if we have a linear density-exposure curve. It is plotted this way to show the detail over the entire range of

exposure, because Figure 4.1 shows that the density-exposure curve is not linear. Although preflashing linearizes the H-D curve, it does not change the linearity of the density-exposure curve, it only increases the ultimate density. Without flashing, we were unable to obtain the peak as shown in Figure 4.2, because the "oscillation" at higher exposure started to become dominant before the peak could be reached. We expect the measured power for the higher order to be greater than the theoretical prediction, due to non-linearity in the density-exposure curve. Detailed plots showing the theoretical efficiency of a 15 micron substrate with different loss factors are shown in Figure 4.3 and 4.4. We see that their shapes are in agreement with those of the experimental data; we estimate that this emulsion has a loss factor of approximately 0.1.

4.4 Some Possible Experiments

In view of the discussion given in the text, major breakthroughs in the use of photographic emulsion are not in the hands of those who are mainly interested in producing better gratings and holograms. The problem is sufficiently well defined that the responsibility is now on the shoulders of chemists who are able to produce thicker, better and more linear emulsions, better reversal baths, better developer for round grains and better desensitizers to preserve the plates. The experiments described here may involve some chemistry, but are still within the grasp of "electrical engineers".

4.4.1 Developer and Chemical treatments

We have studied in Section 1.22 that it is the Redox potential

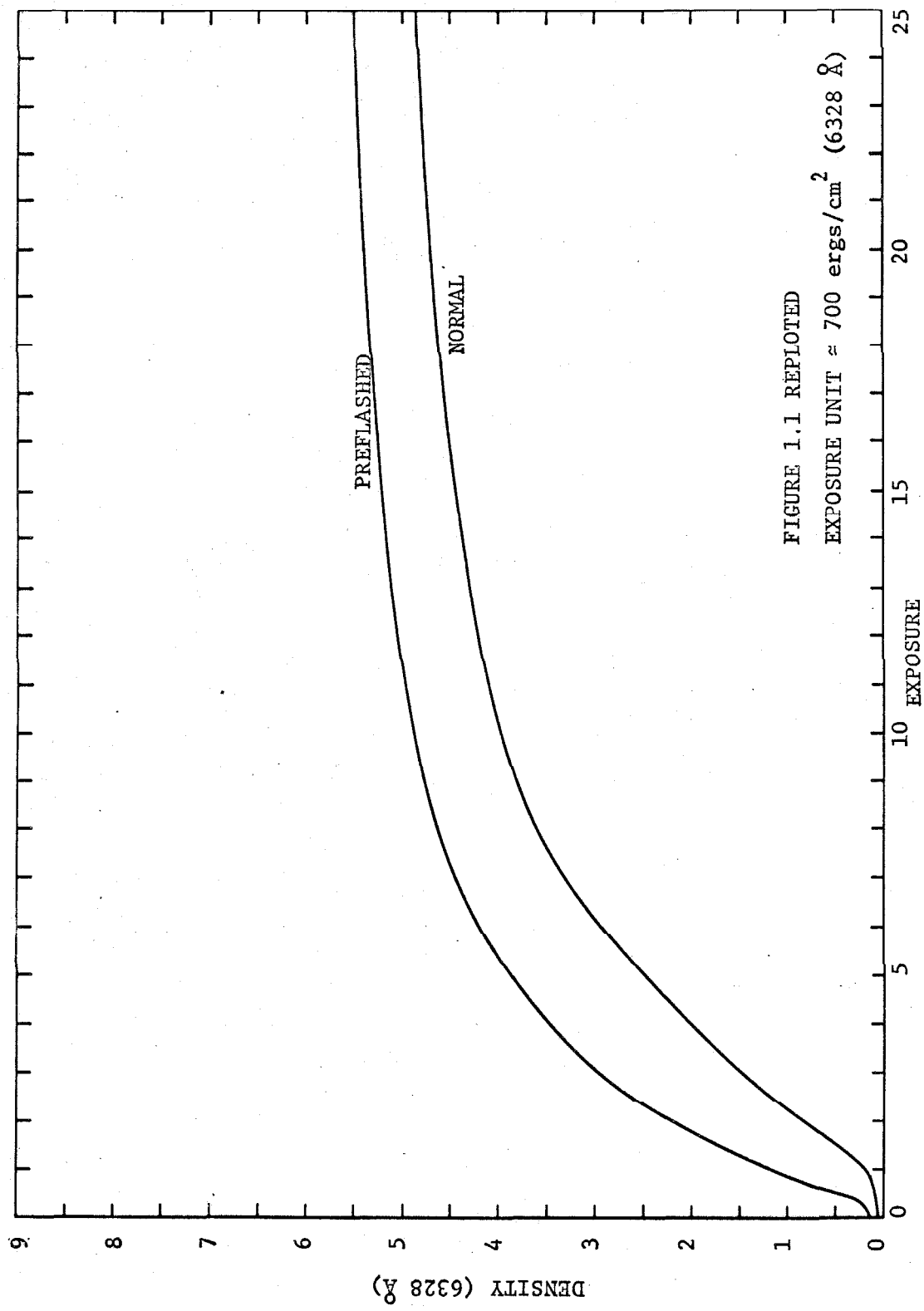

FIGURE 4.1 DENSITY-EXPOSURE OF NORMAL AND PREFLASHED 649F PLATE

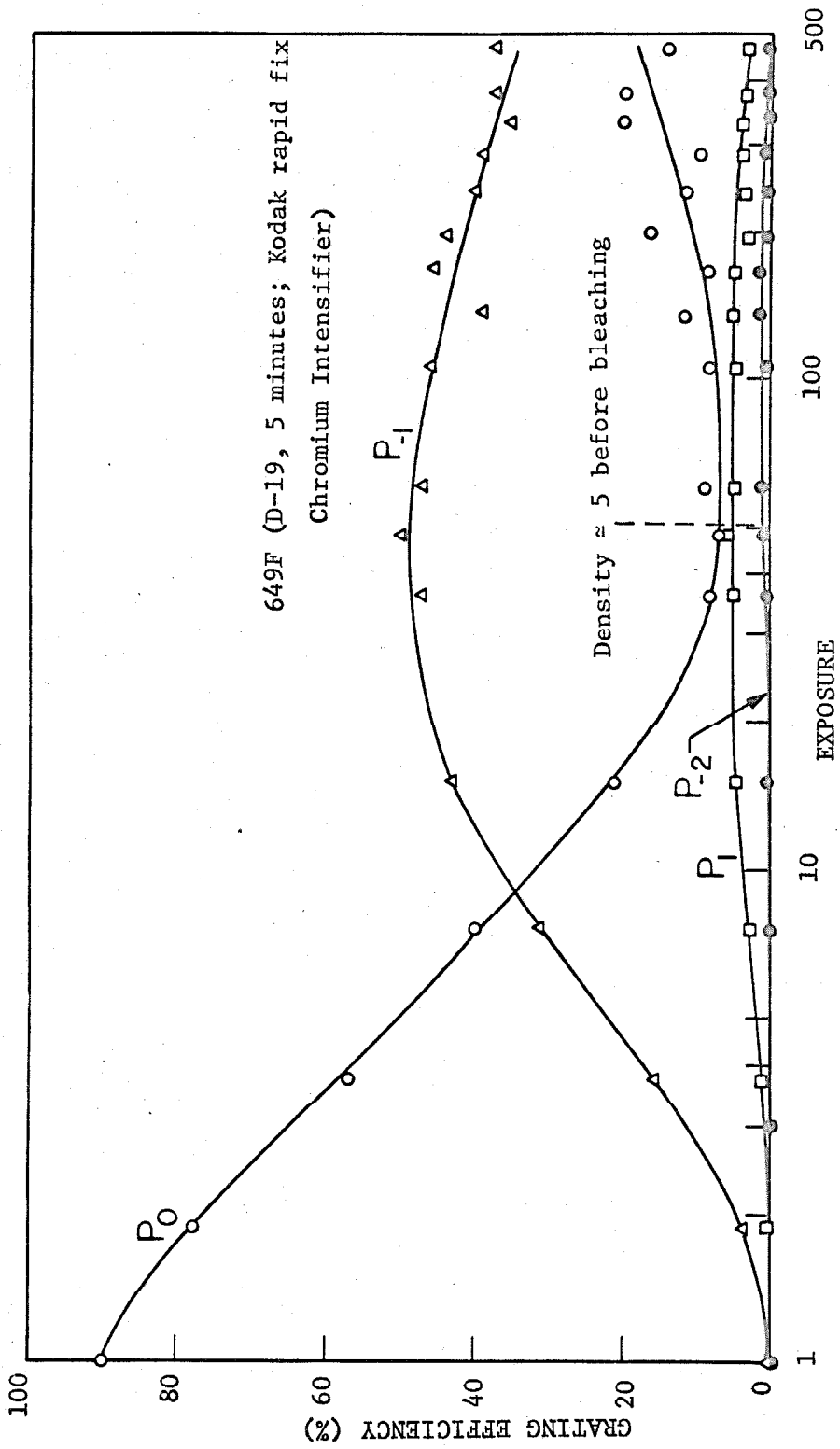

FIGURE 4.2 GRATING EFFICIENCY versus EXPOSURE, 649F PLATE .

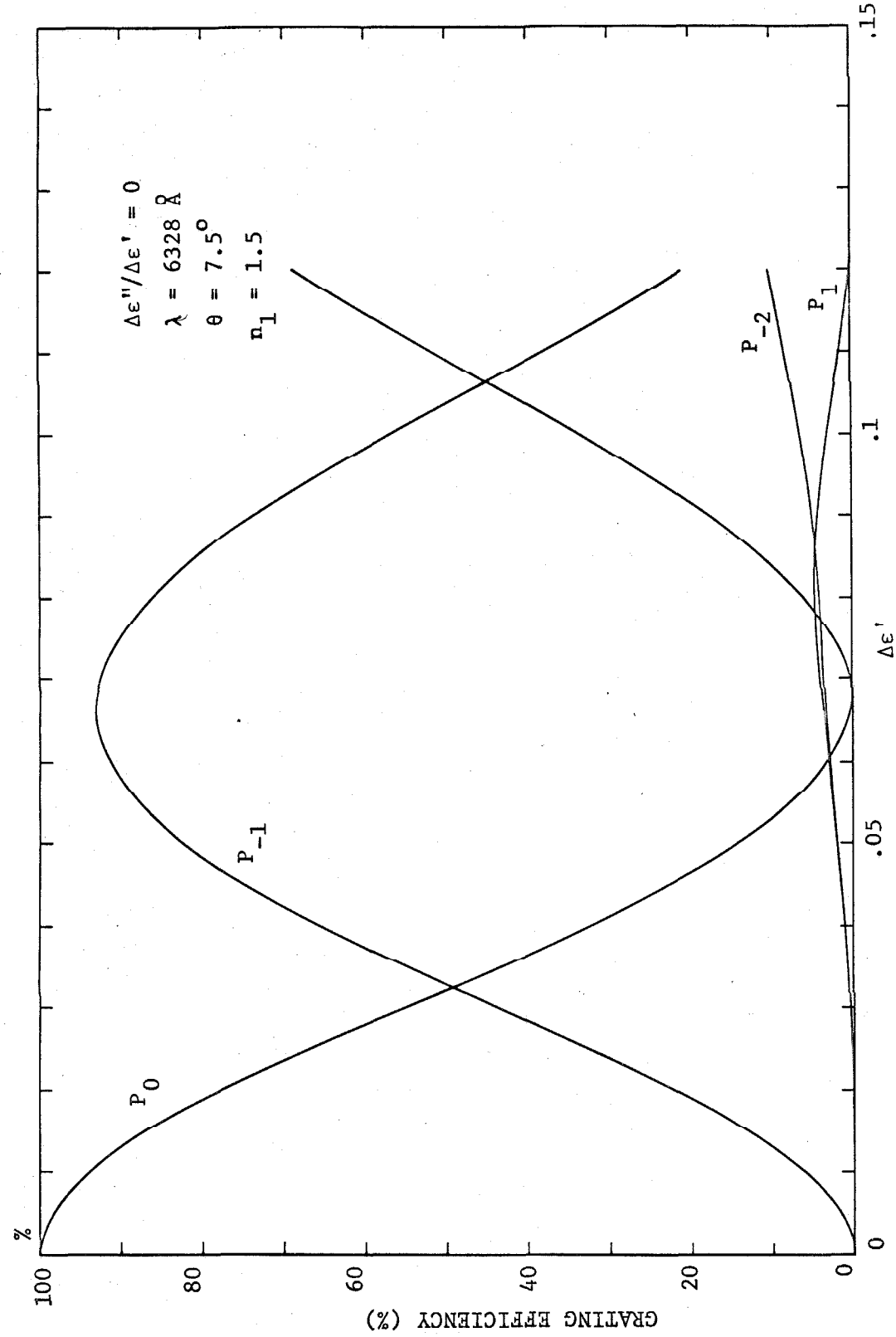

FIGURE 4.3 COMPUTER SOLUTION: FOUR COUPLED WAVE EQUATIONS, L = 15 μ

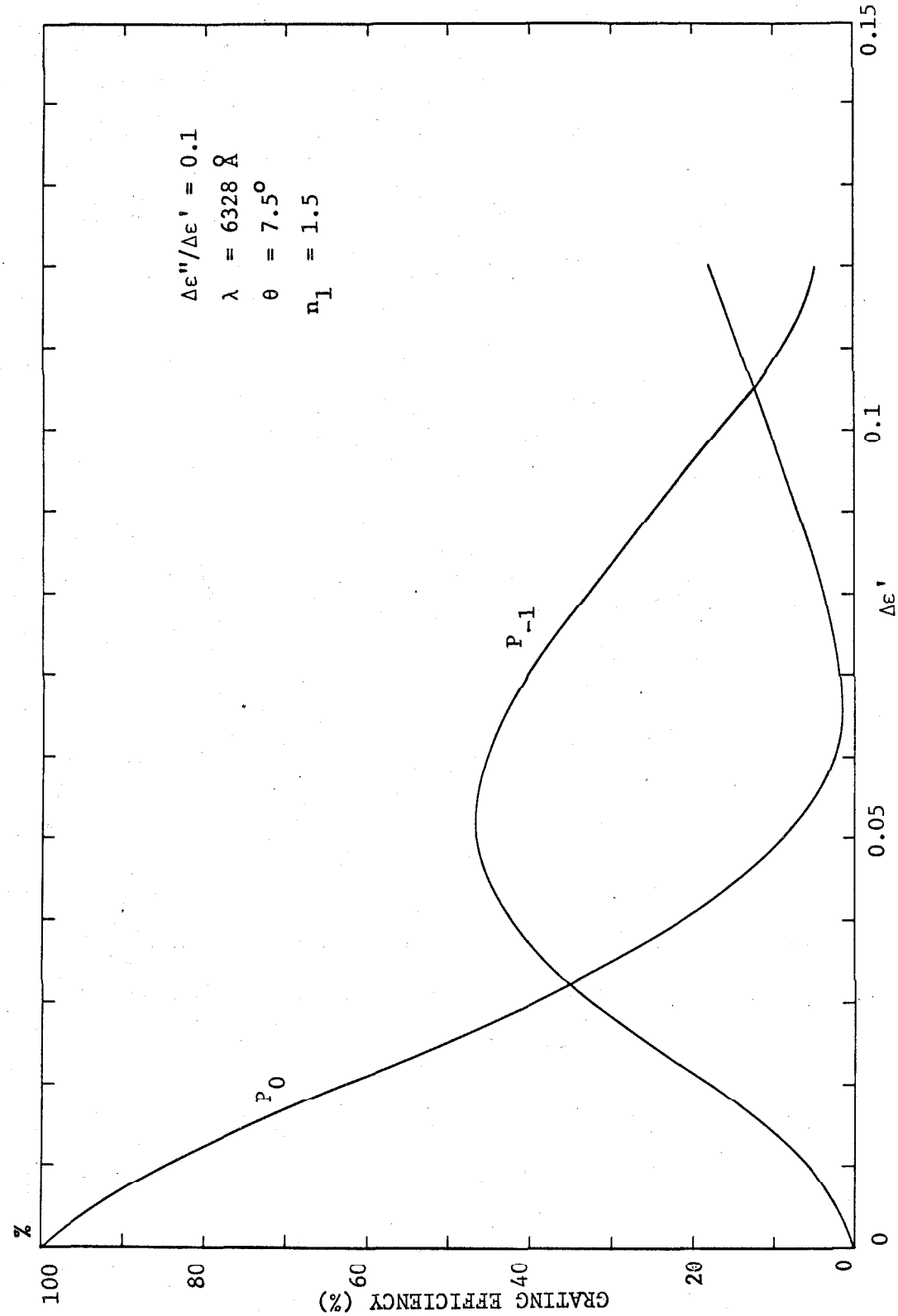

FIGURE 4.4 COMPUTER SOLUTION: FOUR COUPLED WAVE EQUATIONS, L = 15μ

difference between the grains and the developers that is responsible for making the grains long during development. One method of decreasing this potential is to decrease the pH of the developer. This can be achieved by decreasing the amount of sodium carbonate present in D-19. The experiment calls for the extensive use of an electron microscope to correlate the amount of accelerator (sodium carbonate) present, to the shape of the grains.

Another method of making the grains round is by a treatment of KCN of various concentration (4.1). It is uncertain about the final position of the grain relative to its original position. Thus it is necessary to measure the scattering noise by varying the degree of such treatment.

4.4.2 Thickness of the Emulsion

We have shown that by making the grating thicker one is able to obtain a higher ultimate efficiency. We also note that to obtain such efficiency one requires a much smaller index modulation than would be required for thin gratings. This imples that fewer grains need to be present per unit volume. It perhaps offers an additional advantage of reducing noise introduced by multiple scattering between grains. On the other hand, a thick emulsion presents problems in uniform development. Thus an optimum thickness should be determined by experimentation.

4.1 T. H. James, Photographic Science and Engineering 9, 127 (1965).

4.4.3 Improvement of the Modulation Transfer Function.

The possibility of improving the MTF discussed in Chapter Two merits attention. From the simple analytical basis for such improvement we have indicated a different amount of compensation is required for each spatial frequency. In practice one must also take into account the exposure, because of the diffusion of light which causes turbidity. It is necessary to determine the amount of compensation for a given spatial frequency and exposure.

CHAPTER 5

CONCLUSIONS

Emphasis is placed upon photographic emulsion as the medium for producing dielectric gratings, but the treatment is general and includes any material that can have an internal modulation of the refractive index. Three topics are treated: the effective dielectric constant of the emulsion, the diffraction of light by dielectric gratings, and the techniques for producing gratings with high efficiency and good resolution.

The photographic emulsion is treated as an artificially loaded material, i.e., as a suspension of grains in a gelatin base. A Mie scattering theory analysis is used and the effect of adjacent scatterers on the local field is accounted for by the Lorentz-Lorenz relation. The optical density of the emulsion is shown to be proportional to the number of grains present. The effective index variation after bleaching is proportional to the pre-bleached optical density, which implies that the emulsion should have a linear density vs. exposure curve to effect a sinusoidally modulated index of refraction. A relation between the modulation transfer function (MTF) of bleached (M') and unbleached (M) emulsion is derived. It is found that

$$M' \propto \log_{10}[(1+M)/(1-M)]$$

Means for improvement of the MTF is also obtained analytically.

The diffraction of light by a dielectric grating is analyzed using the Raman-Nath formalism which is generalized to include loss.

Graphs are presented showing the diffraction efficiency versus the index modulation for a wide range of thicknesses and loss. The peak efficiency for arbitrary emulsion thickness can be obtained from measurements at a specific thickness by using Figure 3.13. The conclusion is reached that presently available emulsion should be made thicker, preferably in the 20-30 micron range.

The processing techniques of photographic emulsion are emphasized and the merits of various bleaches are evaluated. It is found that resolution can be increased by using a reversal process. The dielectric grains in an emulsion processed this way are round in shape. A desensitizing dye can be used to stabilize the grains and a method of extending the dynamic range of the photographic emulsion is found using a pre-flashing exposure technique.

It is hoped that with the results obtained and the recommendations made, this work may serve as a guide-line for the development of more suitable materials for holographic recording.